Recent Advances in High-Pressure Techniques at the LVP Facilities at GSECARS (APS)

Y. Wang, N. Nishiyama*, T. Sanehira, M. Rivers, S. Sutton

The University of Chicago
GeoSoilEnviroCARS Sector at the Advanced Photon Source
** Now at Geodynamics Research Center, Ehime University, Japan*

(Supported by US National Science Foundation and US Dept. of Energy)

Outline

- Ultrasonics at high P and T
  - Acoustic velocities and P-V-T equations of state
- Crystallography at High P and T
  - CAESAR diffraction for structural refinements
- Melt Properties
  - Viscosities
  - Melting curve determination using X-ray transparent anvils
- Rheology at high P and T
  - Flow law determination
  - Lattice preferred orientation and slip systems
- New developments – towards megabar
  - Modified cubic anvil apparatus
  - DDIA-30
- Conclusions

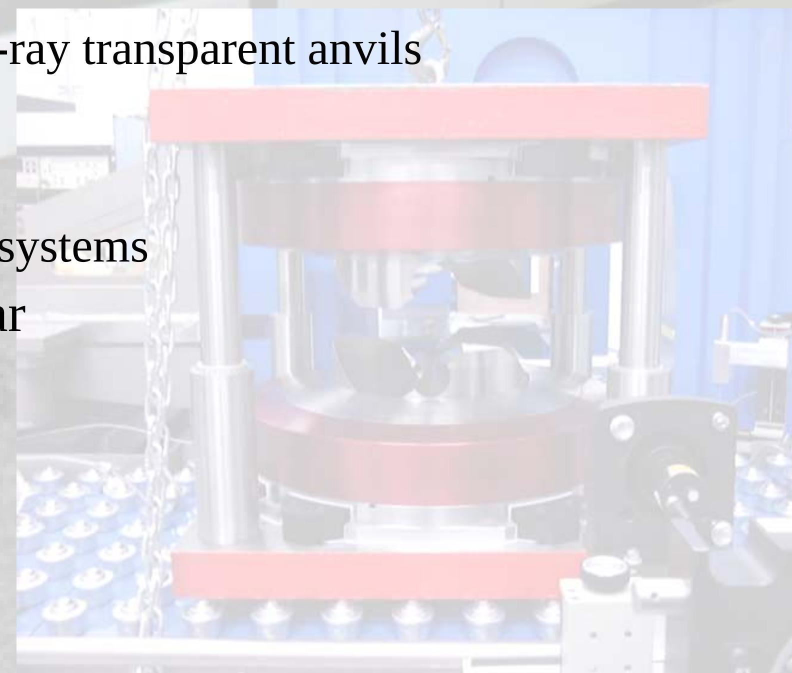

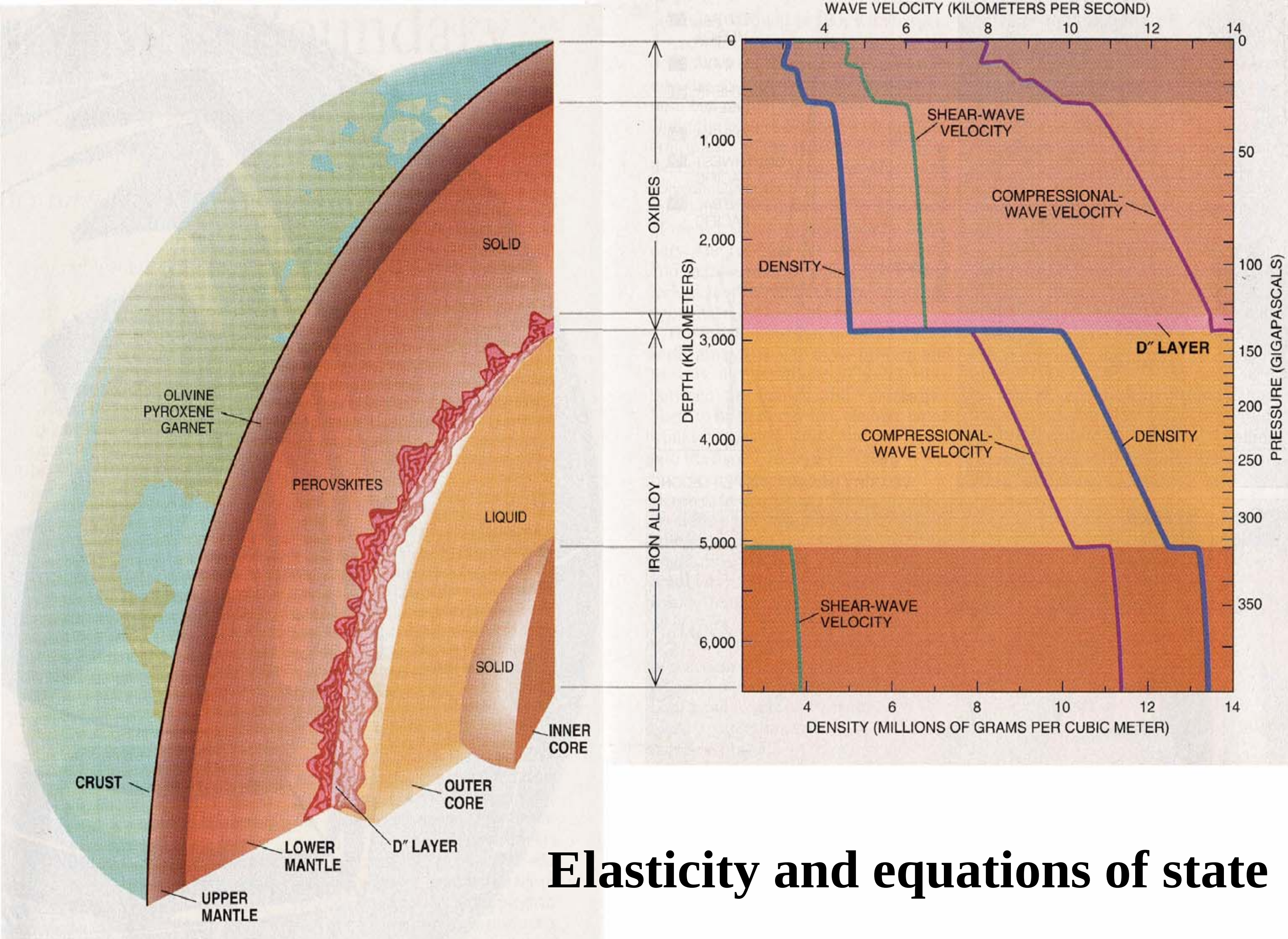

Elasticity and equations of state

P-V-V_P-V_S-T-L Measurements to 25 GPa and 1600 K (B. Li et al., 2006)

(b) Cell assembly

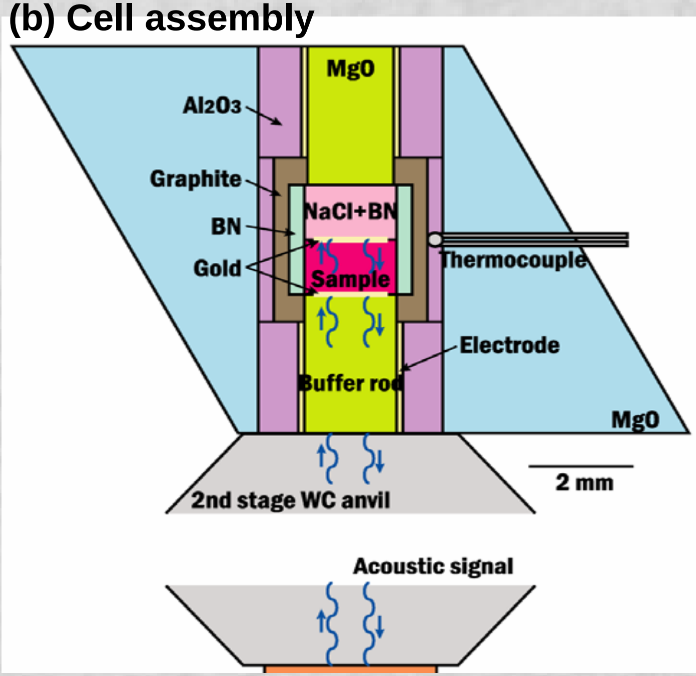

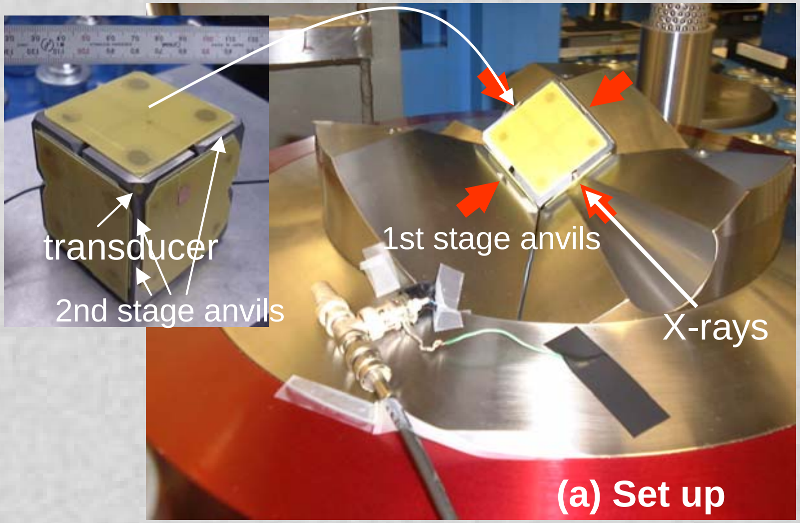

(c) X-ray diffraction

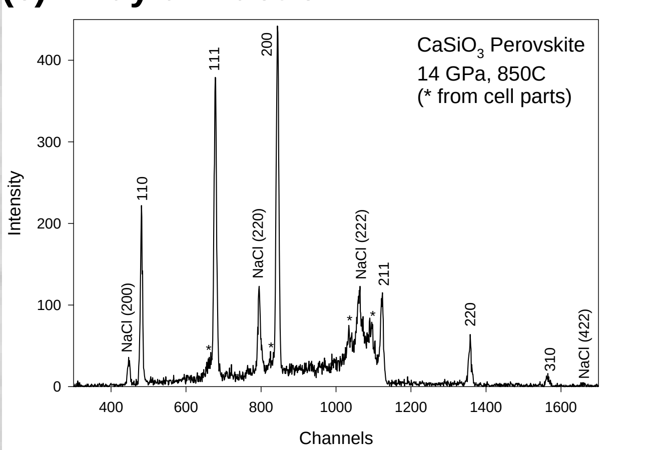

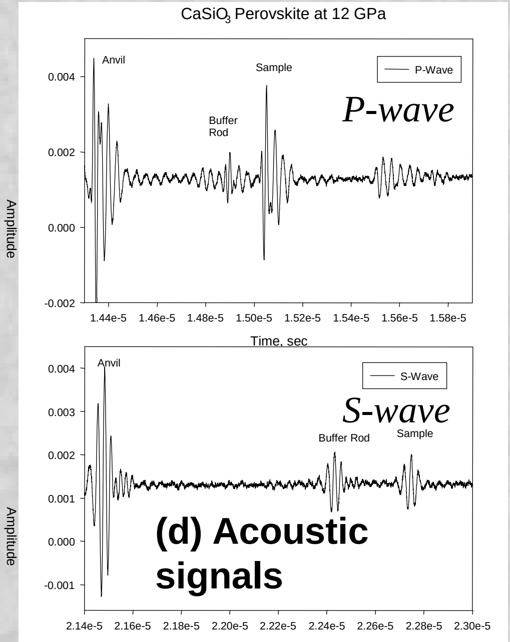

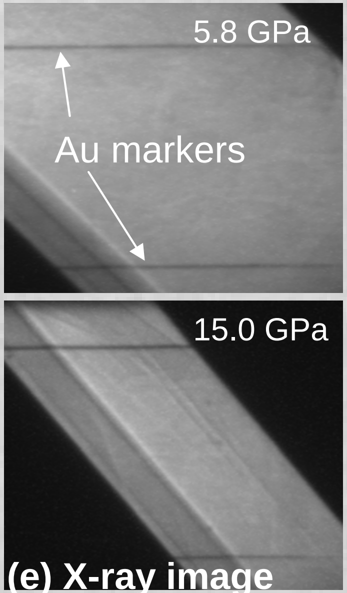

Unquenchable High-Pressure Clinoenstatite

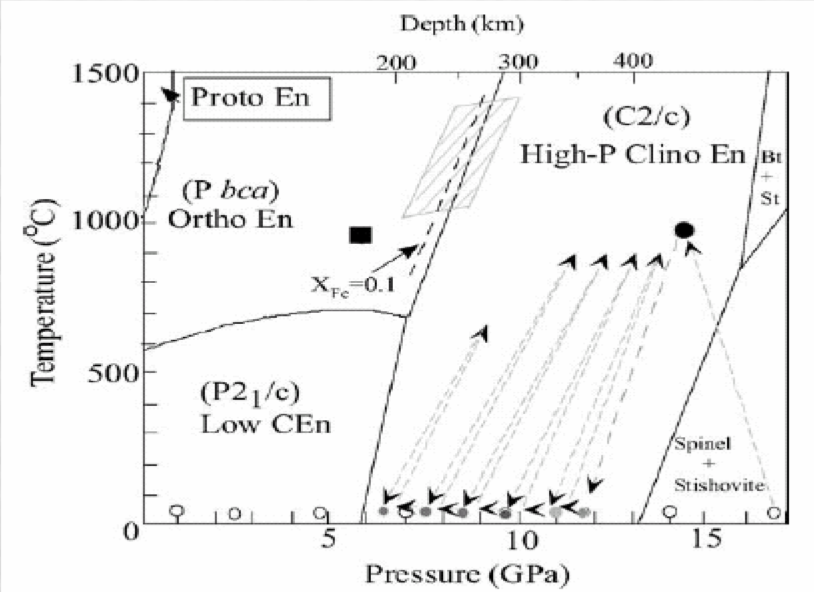

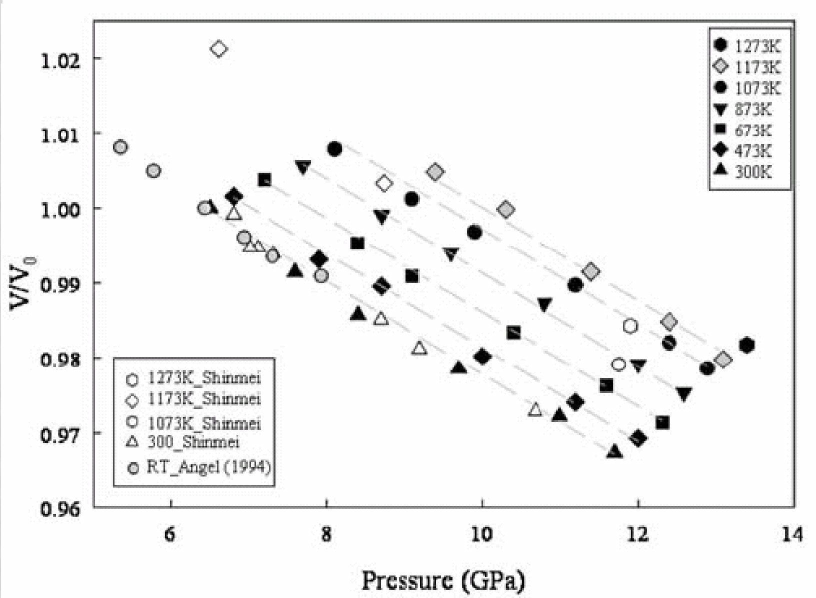

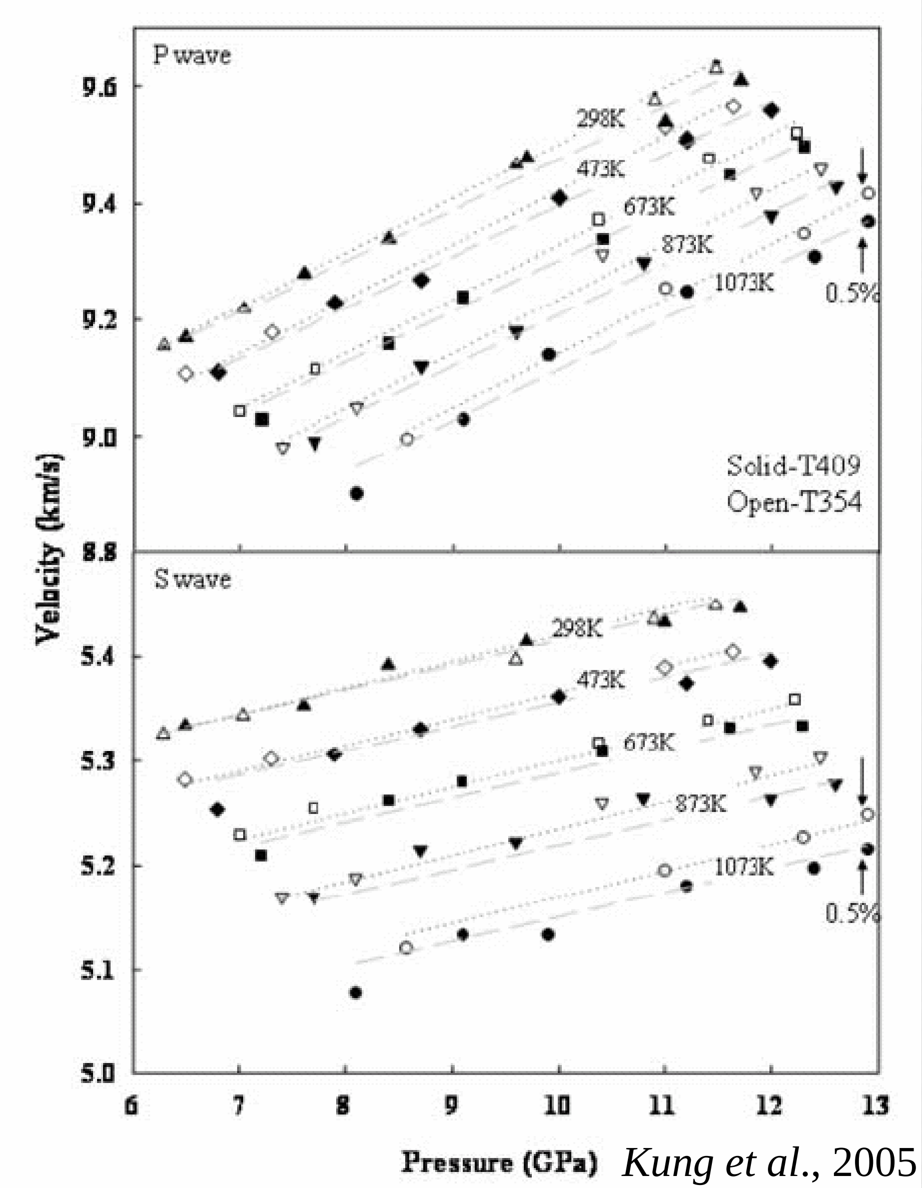

Kung et al., 2005

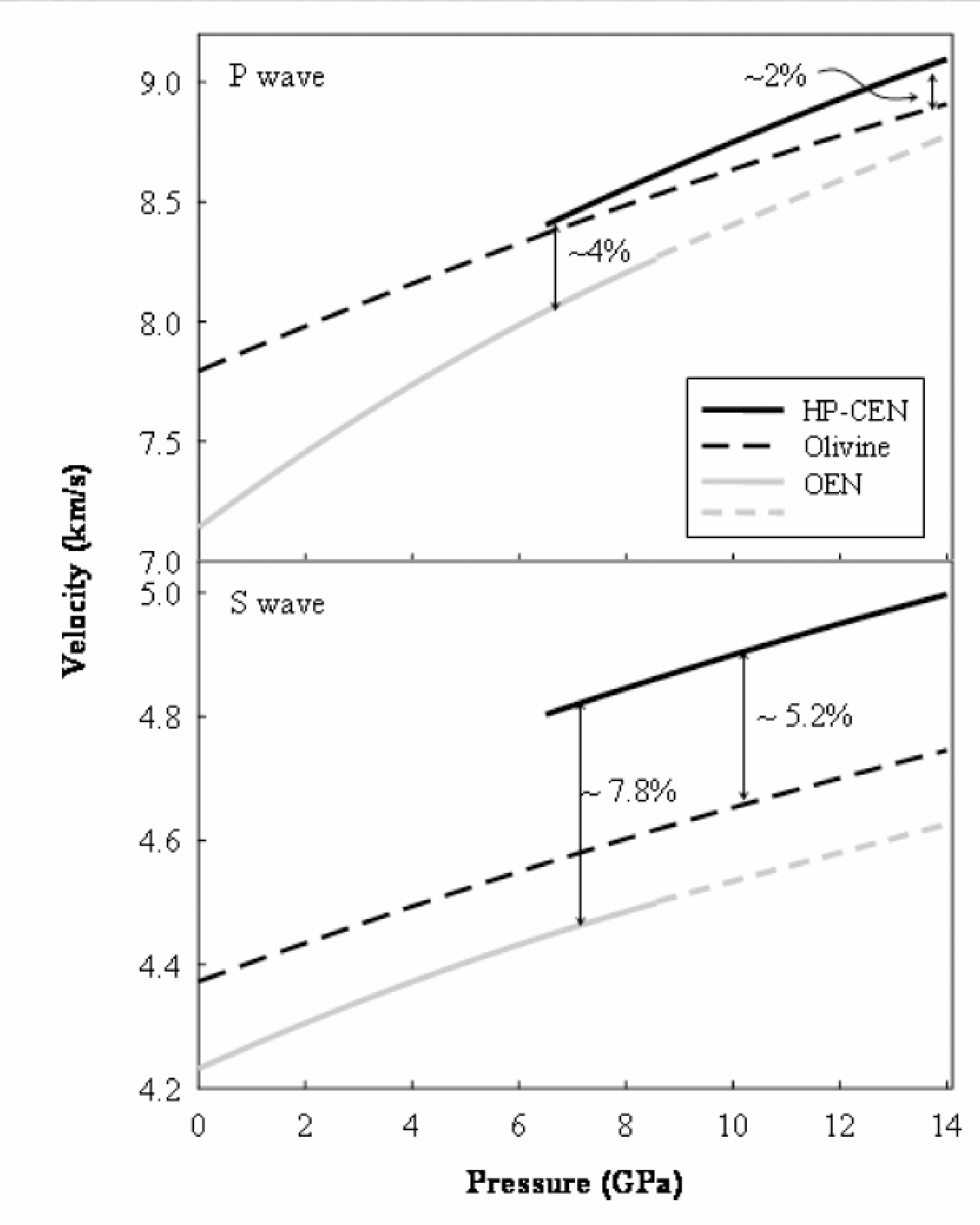

Kung et al., GRL, 2005

CAESAR diffraction and high P-T crystallography

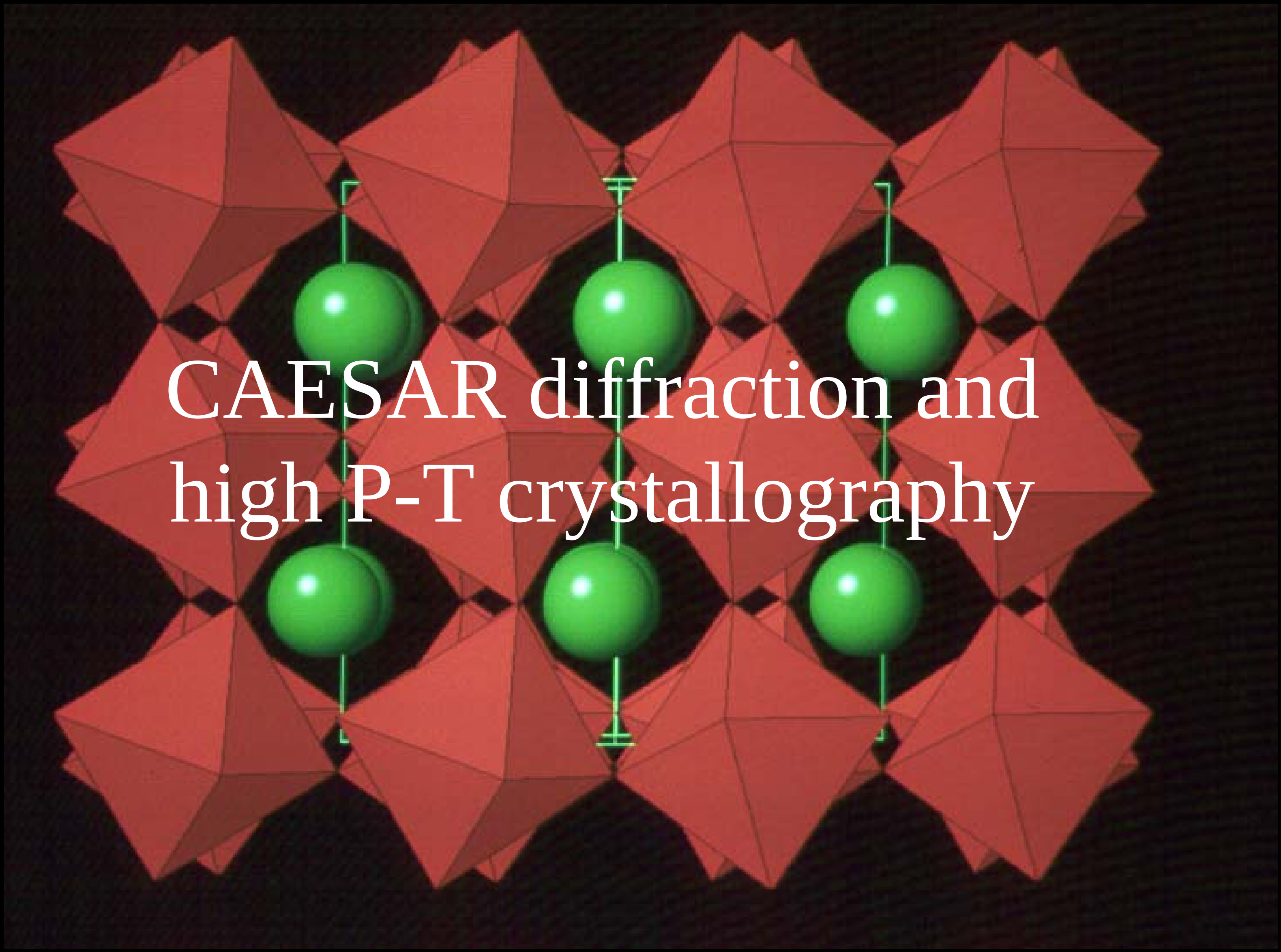

Conventional Step-Scan with Upstream Single-Energy Discrimination

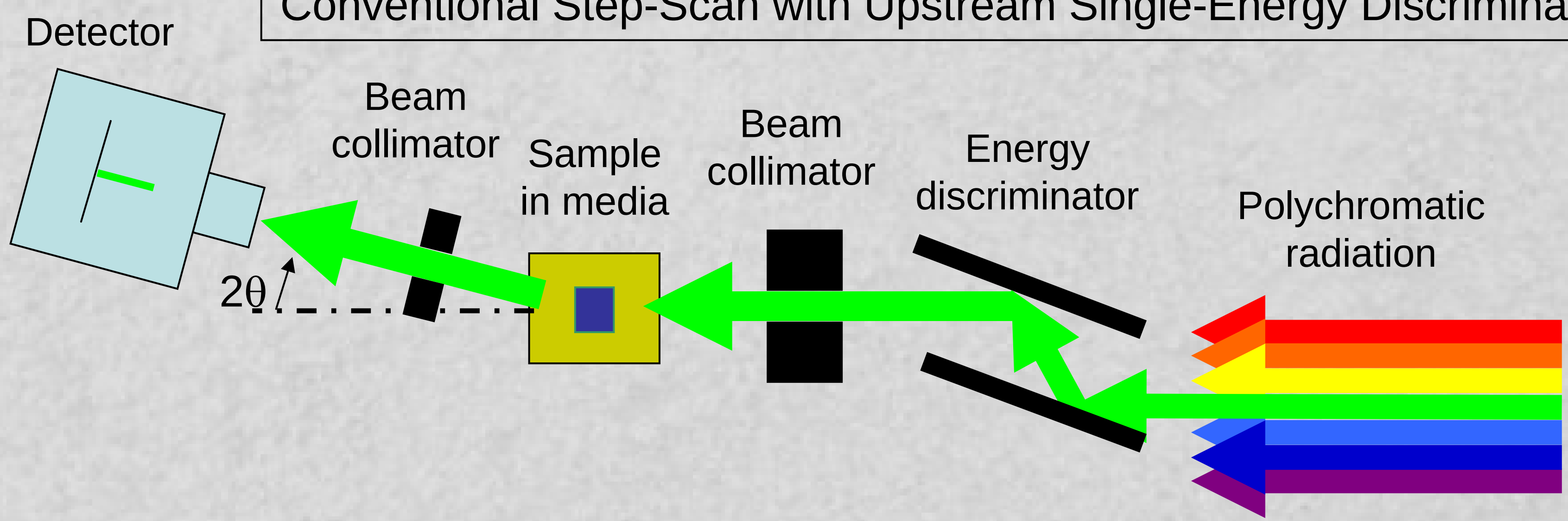

New Step-Scan with Downstream Multi-Energy Discrimination

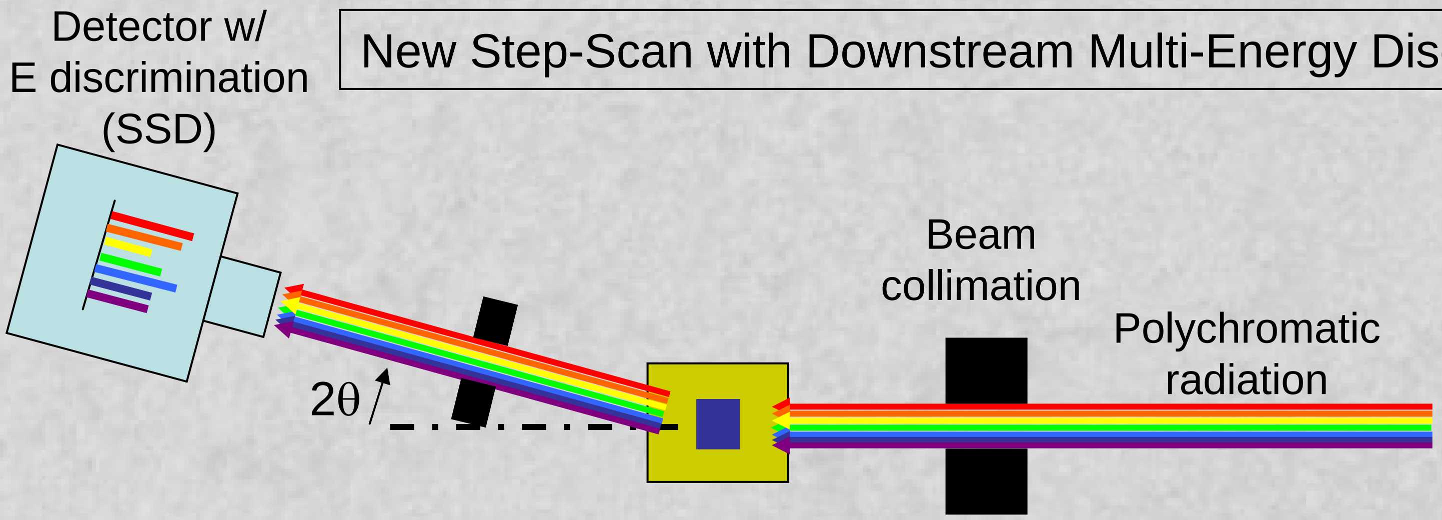

Combined Angle- and Energy-dispersive Structural Analysis and Refinement (CAESAR)

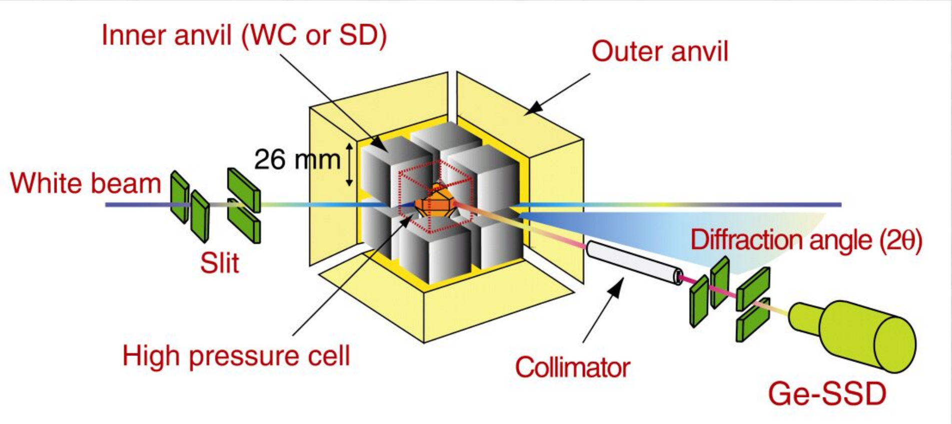

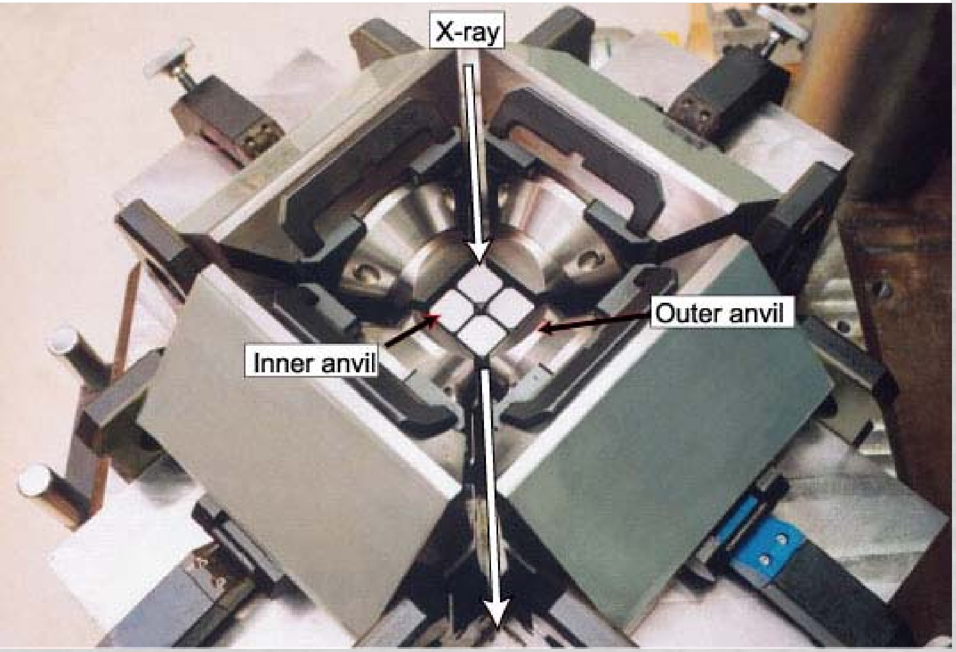

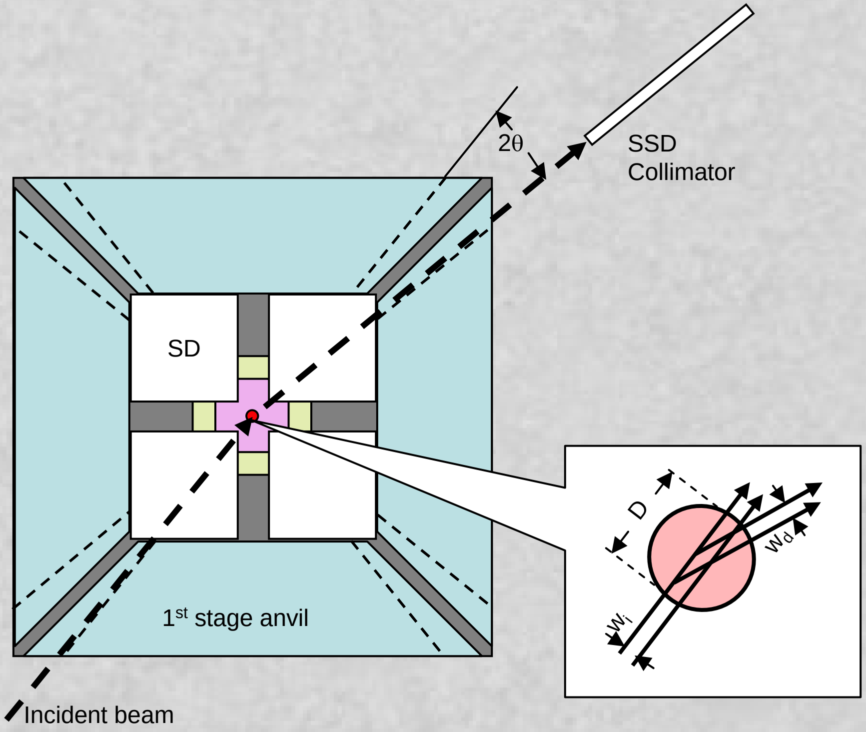

Wang et al., JAC, 2004.

High P-T CAESAR diffraction on $CaSiO_3$ perovskite

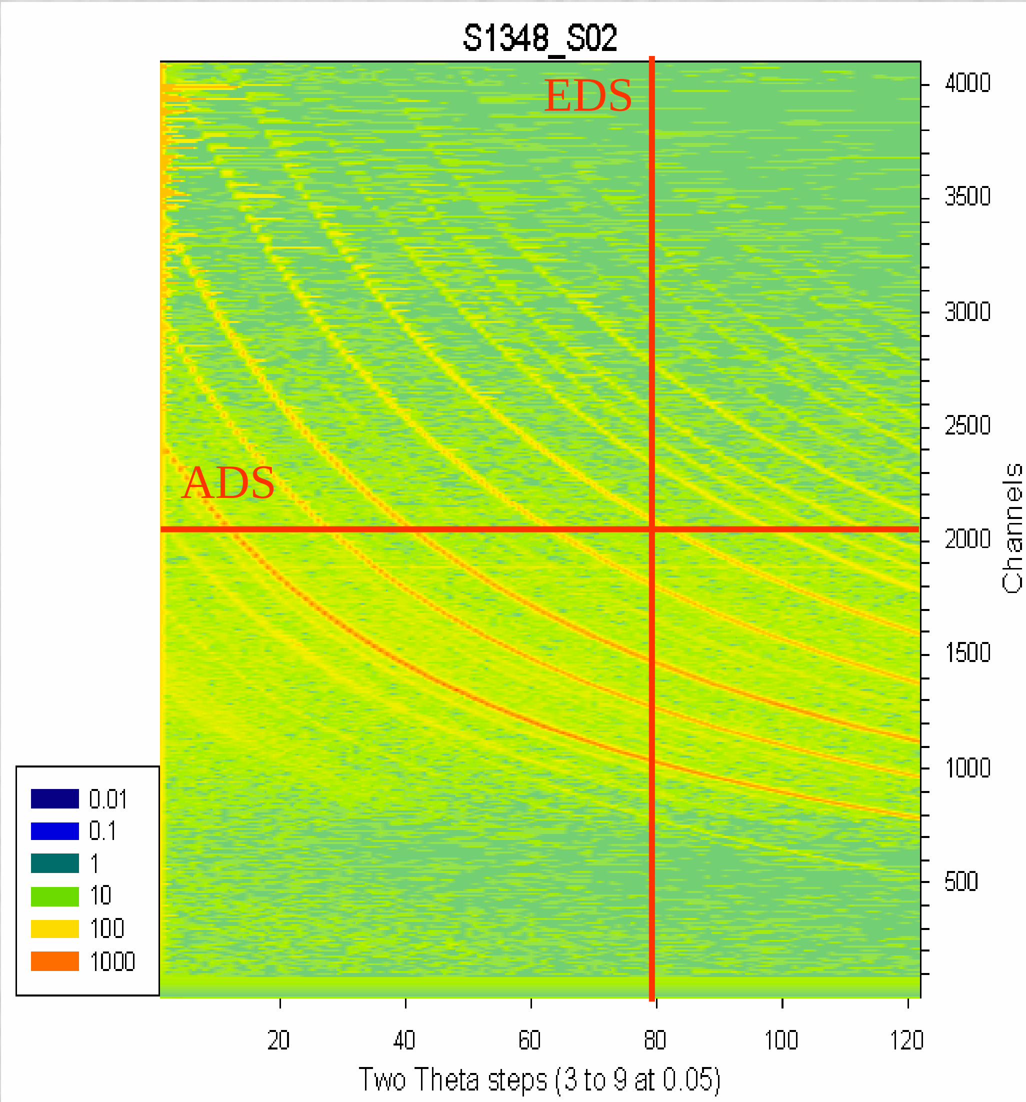

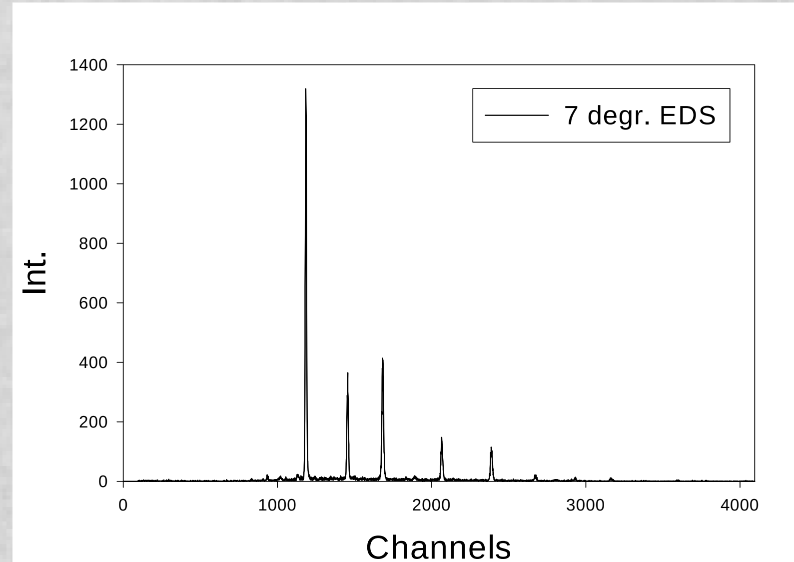

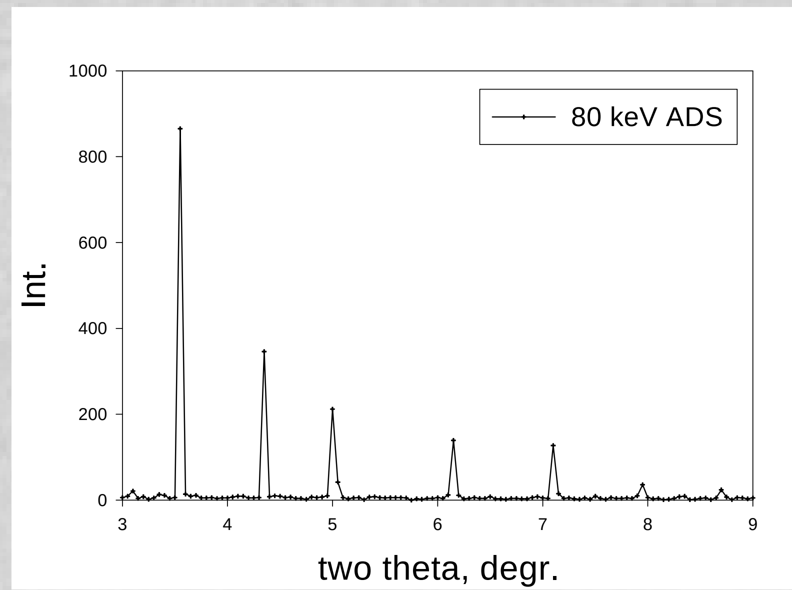

Work conducted at BL04B1, SPring-8

Reitveld refinements at 13 Pa, 1320 K

13.0 GPa, 1320K, Cmcm				
a = 7.1365(7) Ǻ, b = 7.0981(15) Ǻ, c = 7.1163(7) Ǻ, V = 360.479(63) $Ǻ^3$				
Species	x	y	z	Uiso
Ca(1)	0	-0.010(4)	¼	0.012(5)
Ca(2)	0	0.498(6)	¼	0.021(6)
Si(3)	¼	¼	0	0.009(2)
O(4)	0.261(6)	0	0	0.000(6)
O(5)	0	0.237(15)	-0.003(6)	0.028(12)
O(6)	0.270(7)	0.259(12)	¼	0.025(9)
Texture index: 1.7987 (2^{nd} order spherical harmonic)				

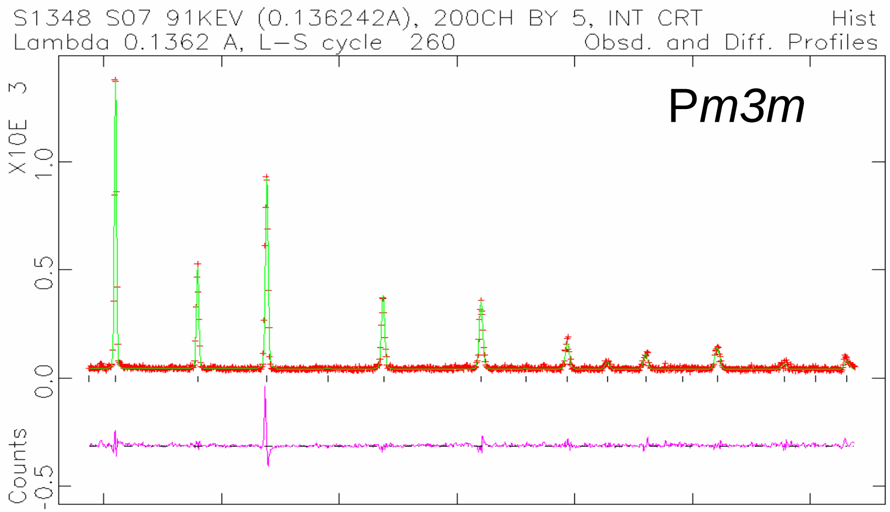

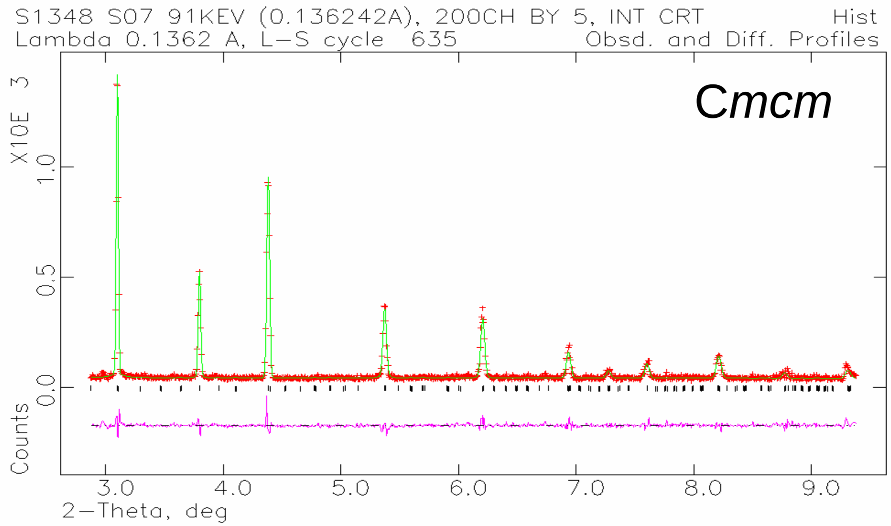

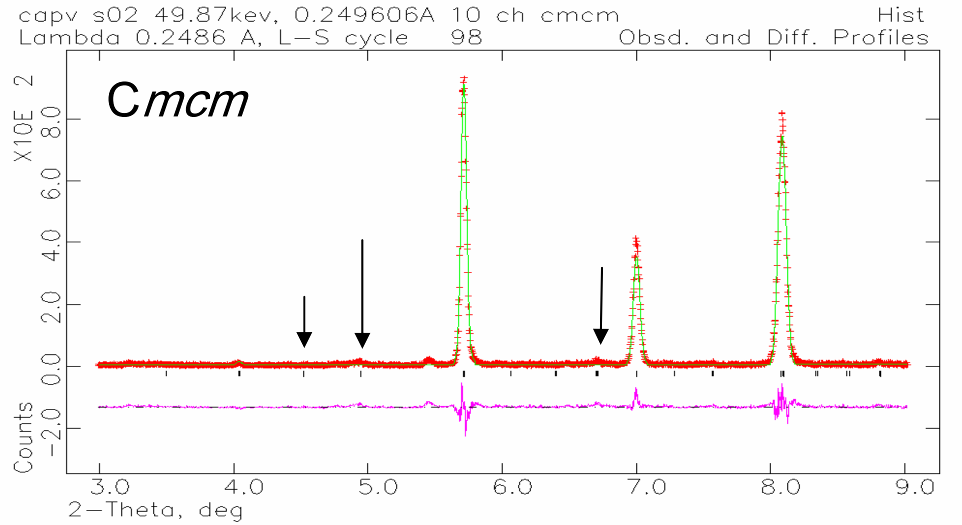

Uchida et al., in prep.

Best Fit: *Cmcm*

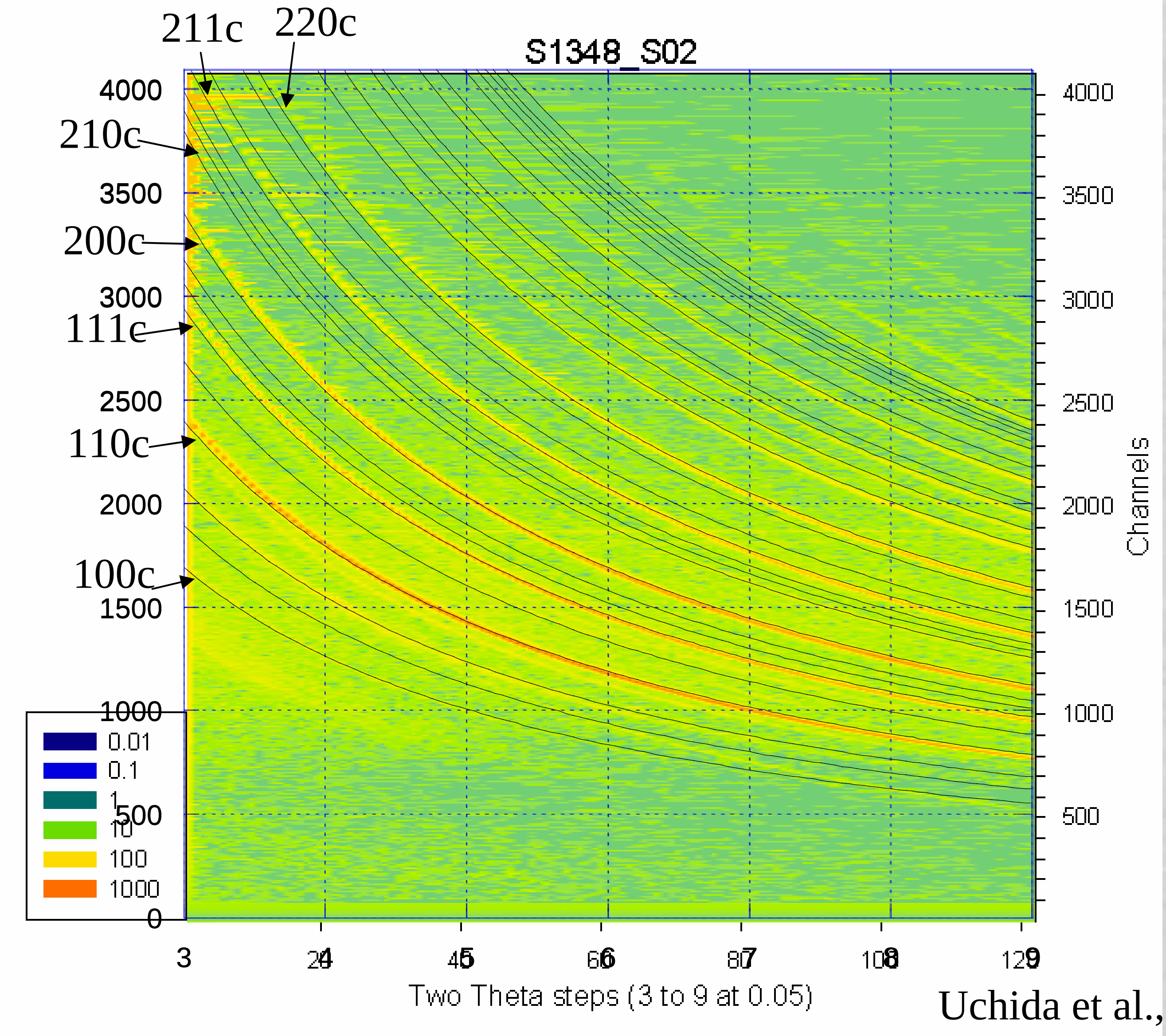

Uchida et al., in prep.

Structural stability

- $CaSiO_3$ perovskite:
  - Non-cubic distortion persists up to 24 GPa and 2050 K
- $CaSiO_3$ + 3wt% Al_2O_3 perovskite:
  - Cubic up to 22 GPa and 2000 K

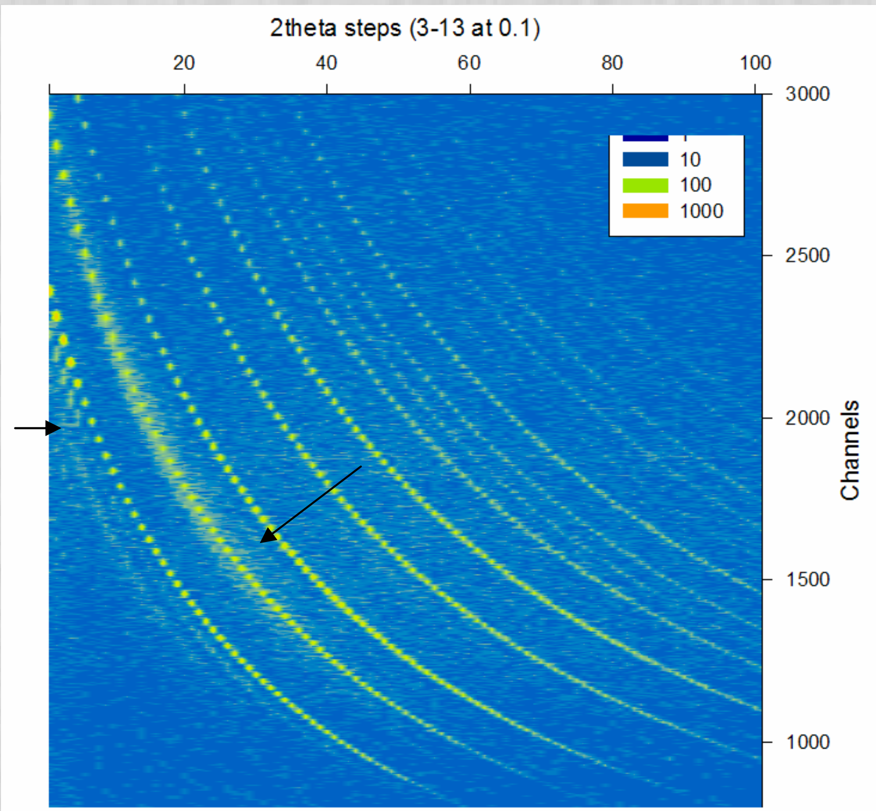

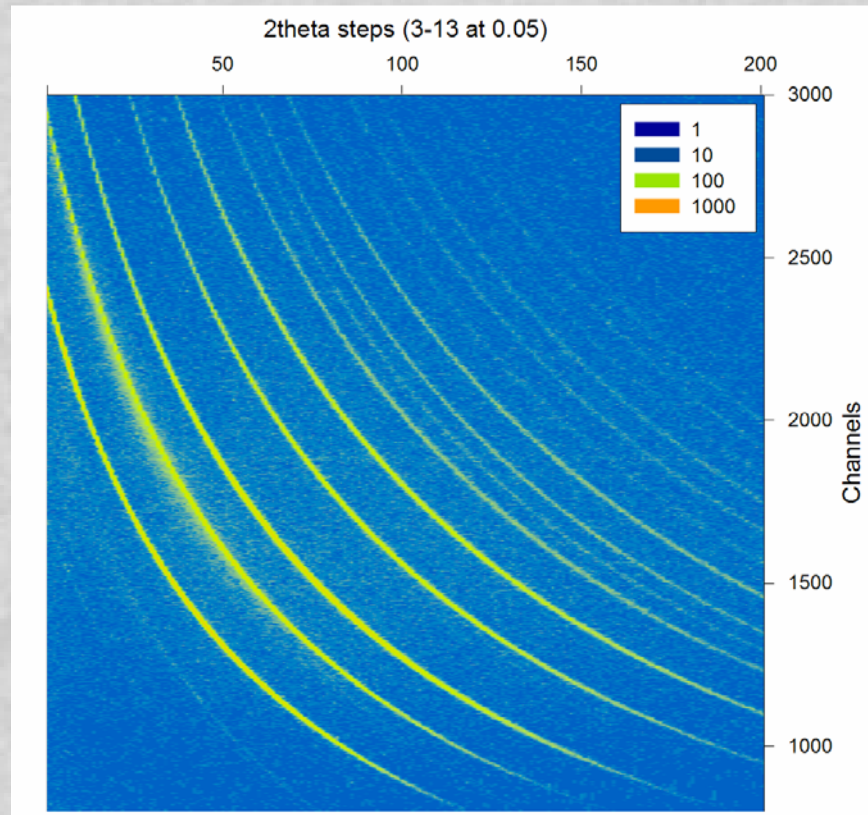

Melt properties

- Viscosity
- Melting curves

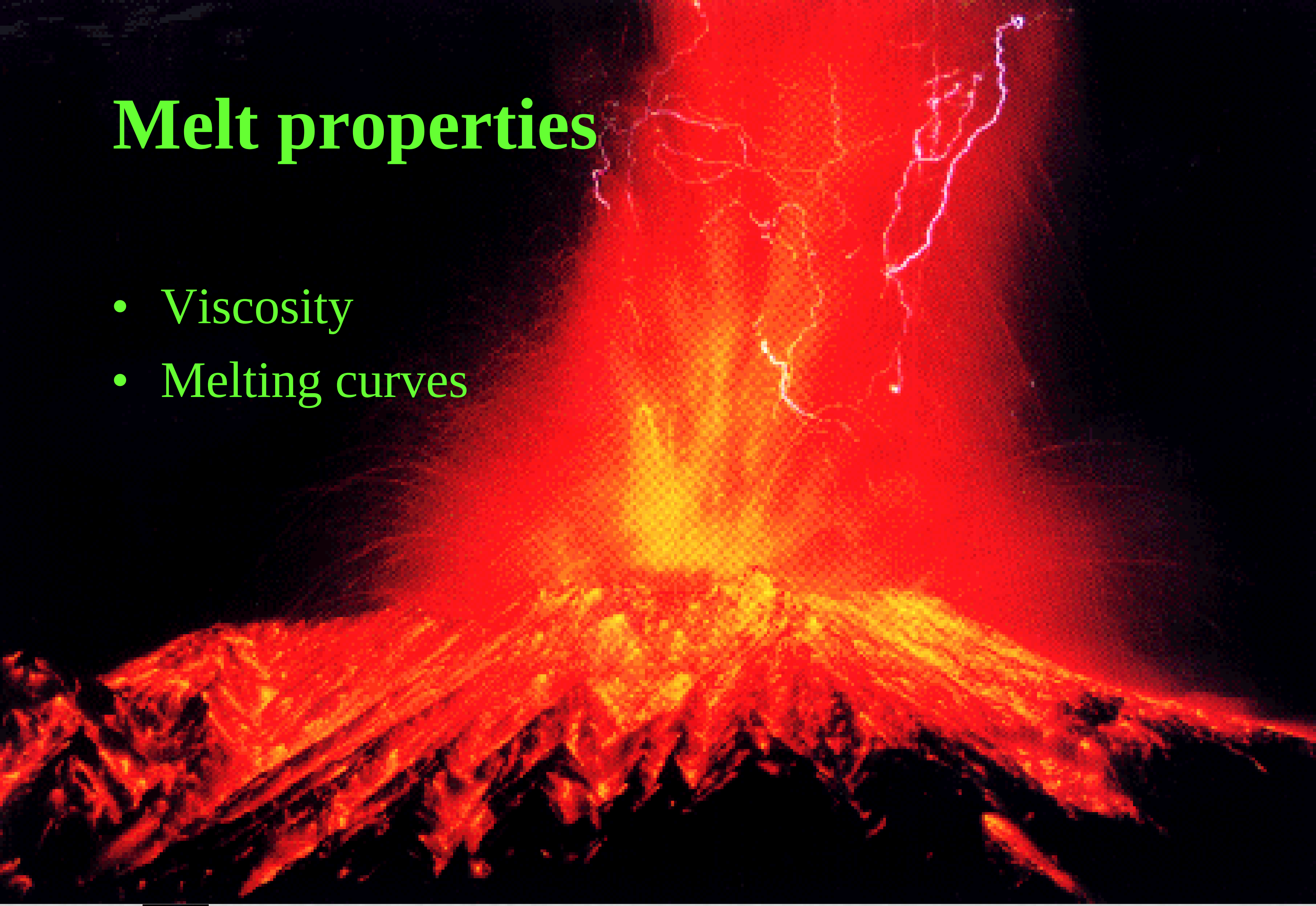

Viscosity of Melts Under High P-T

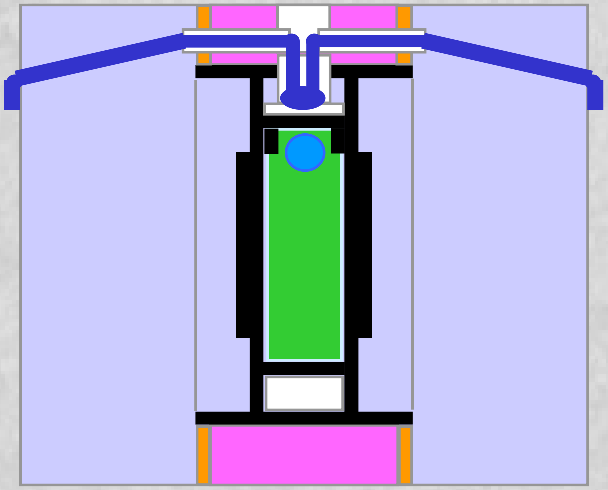

$$\boxed{\sigma = \eta \dot{\varepsilon}}$$

Terminal velocity:

$v_t = (2\,\Delta\rho\, r^2\, g) / (9\,\eta)$

$\Delta\rho = \rho_{sphere} - \rho_{melt}$

r = sphere radius.

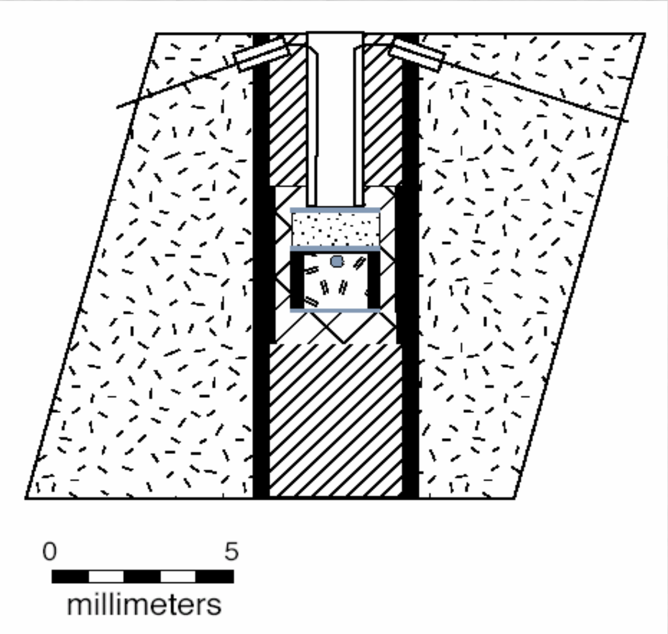

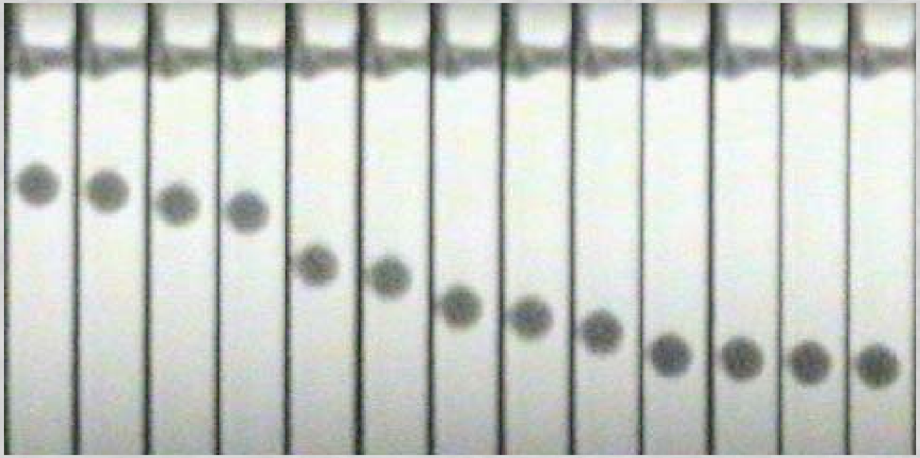

Diopside: Reid et al., unpublished

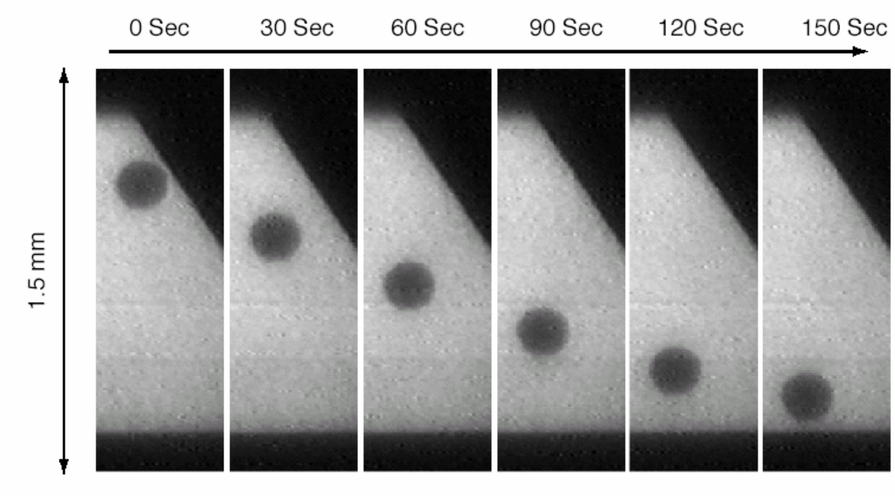

Dacite: Tinker et al., Am Min, in press

Melt viscosity

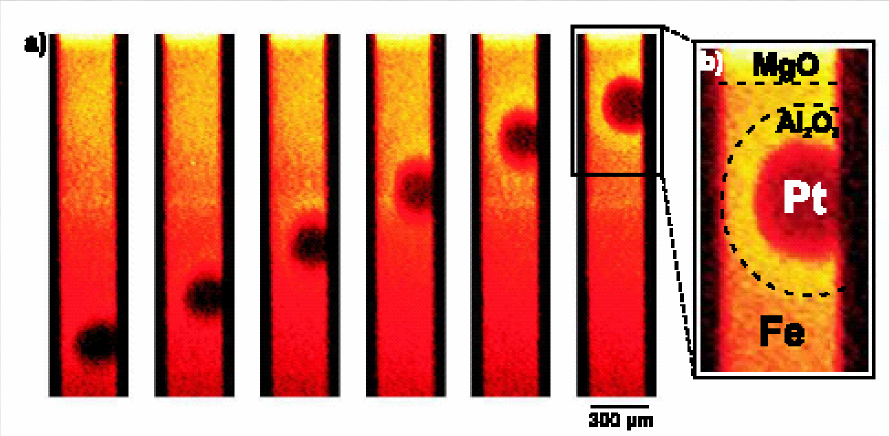

$$\eta = \frac{k_B T}{D(O)\lambda}$$

λ = 2.8 Å diameter of (O^{2-})

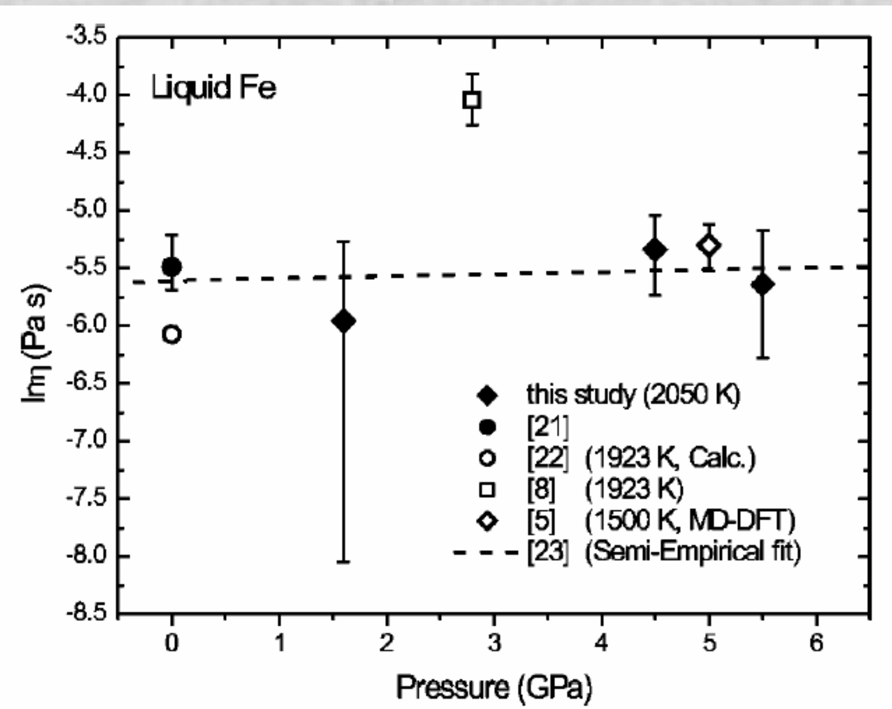

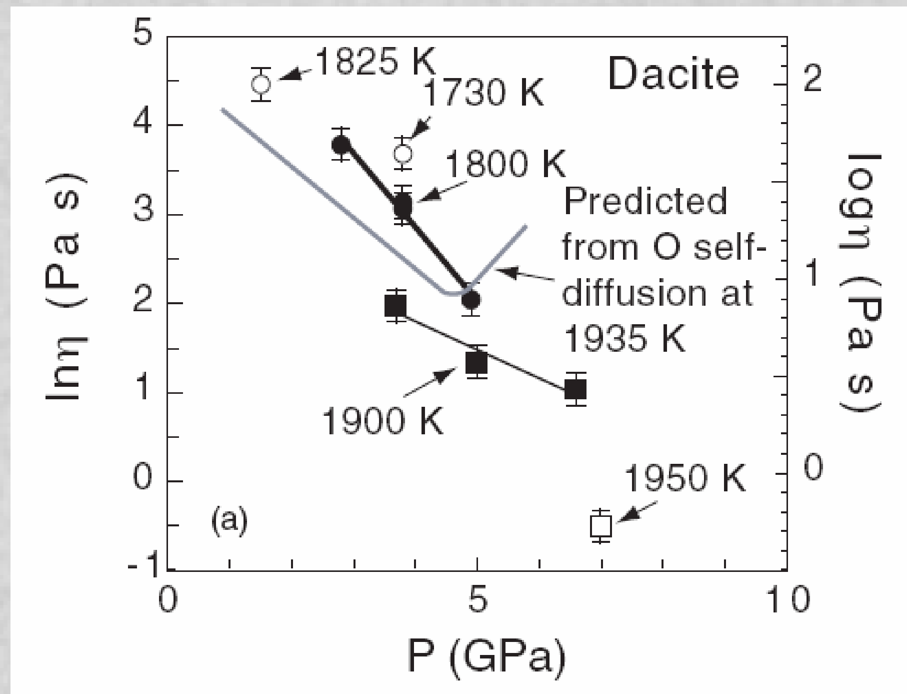

Pure Fe at 2050 K (*Rutter et al.*, PRB'02)

Use X-ray transparent anvils in mono diffraction

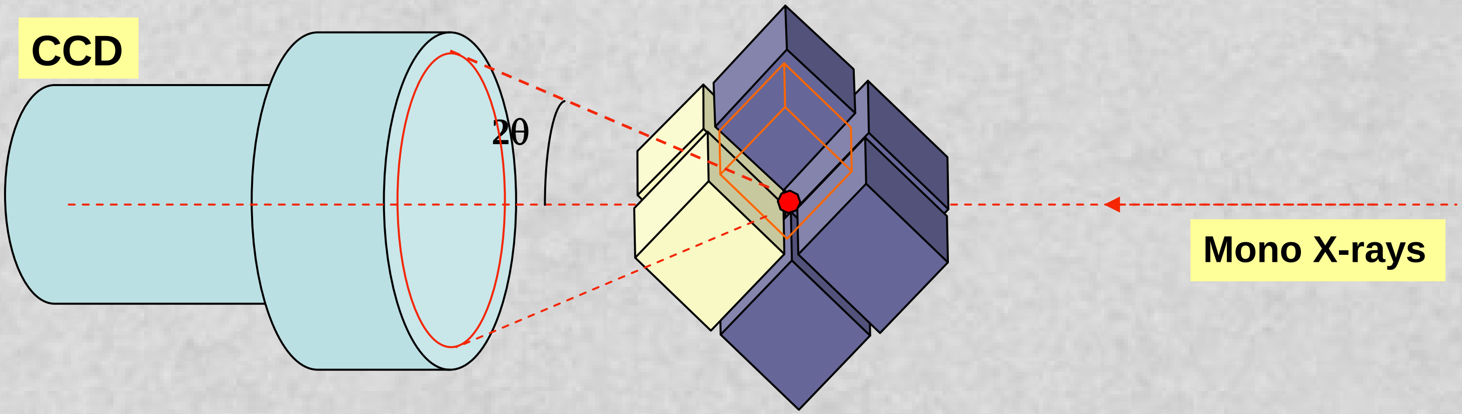

T-Cup, sintered diamond anvils as X-ray windows
2D monochromatic diffraction (ADD)
Record diffraction signal over entire 360° azimuth angle

Si: XI – V – L triple junction

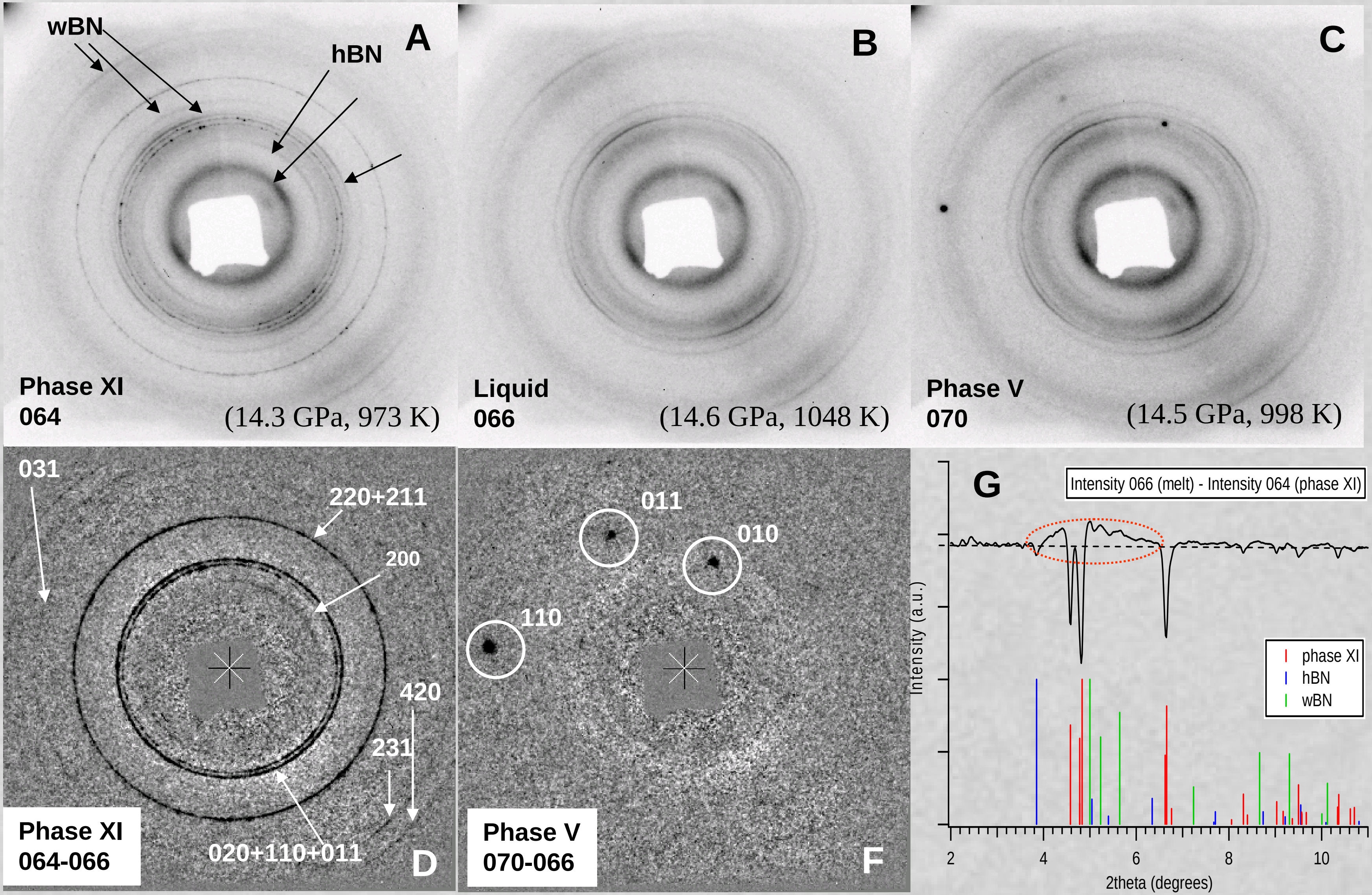

Kubo et al., JPCS, in press

Melting Curve of Si

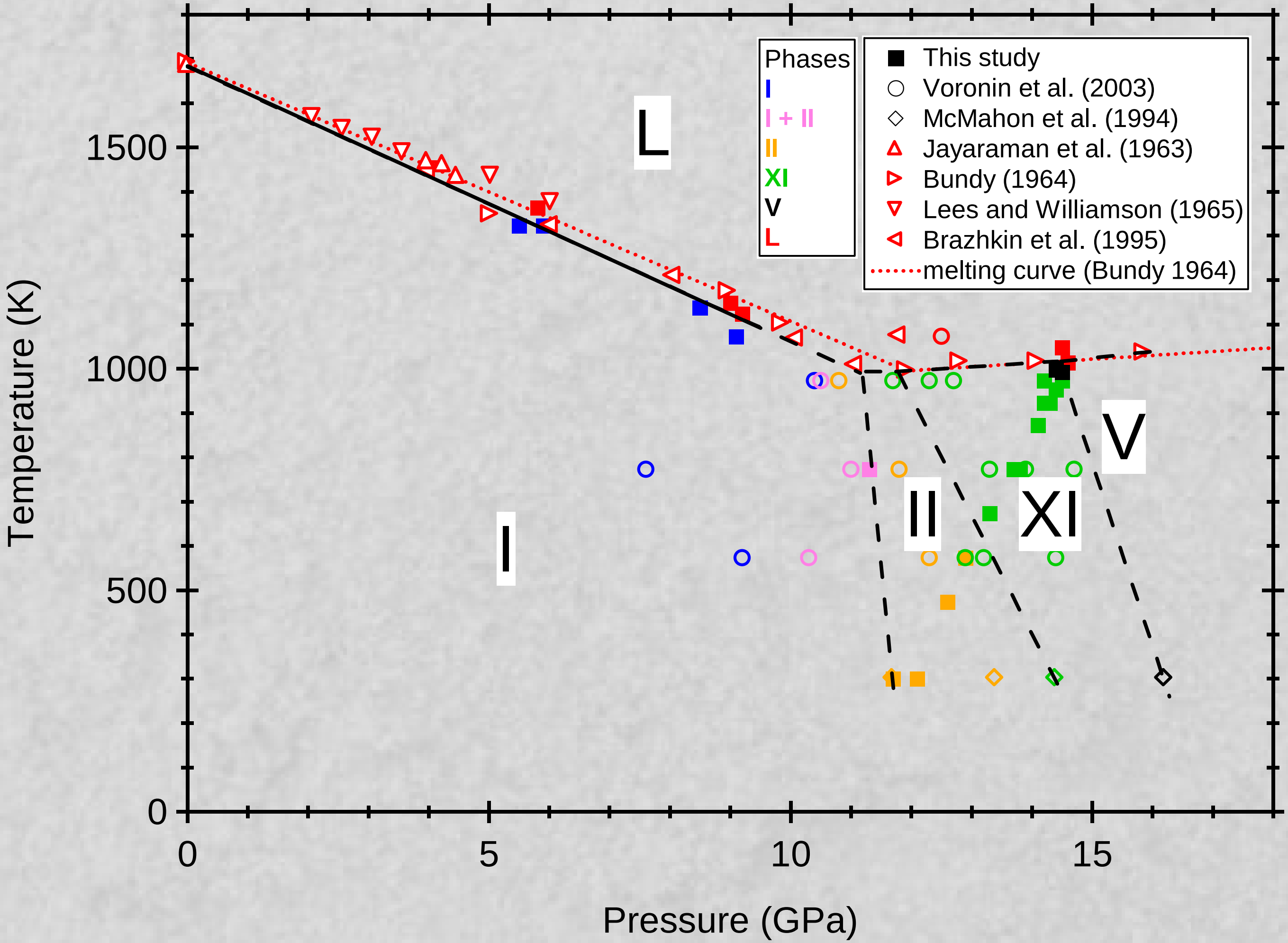

Kubo et al., JPCS, in press

Rheology of earth materials

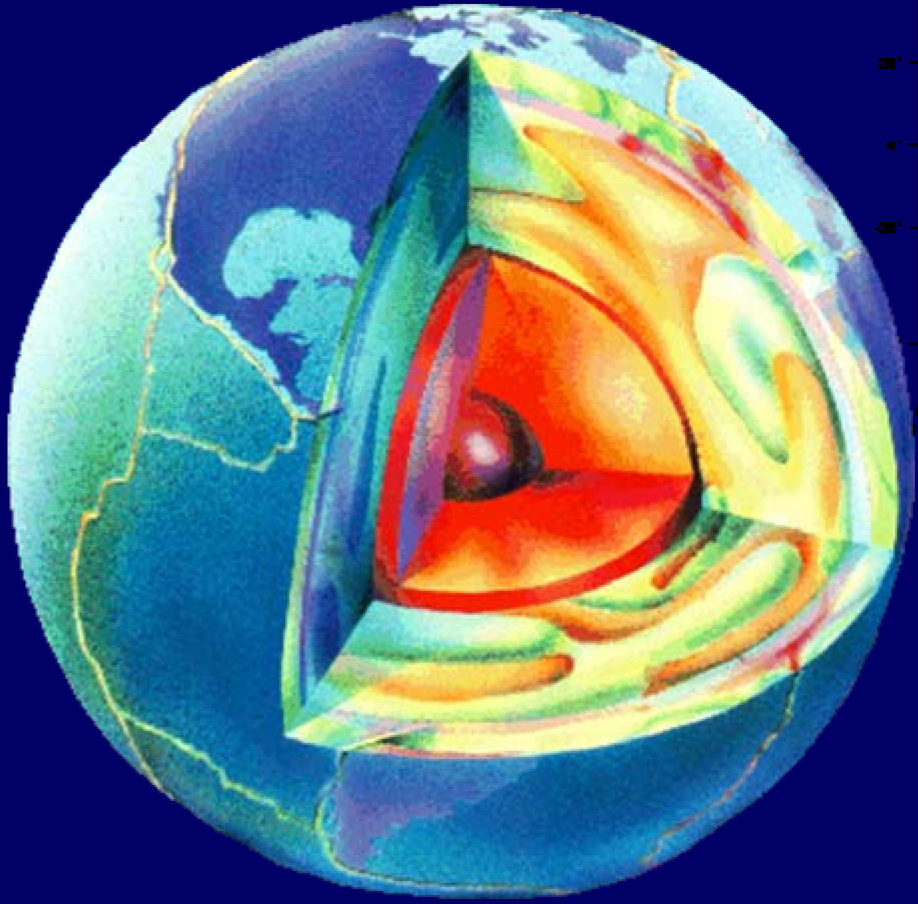

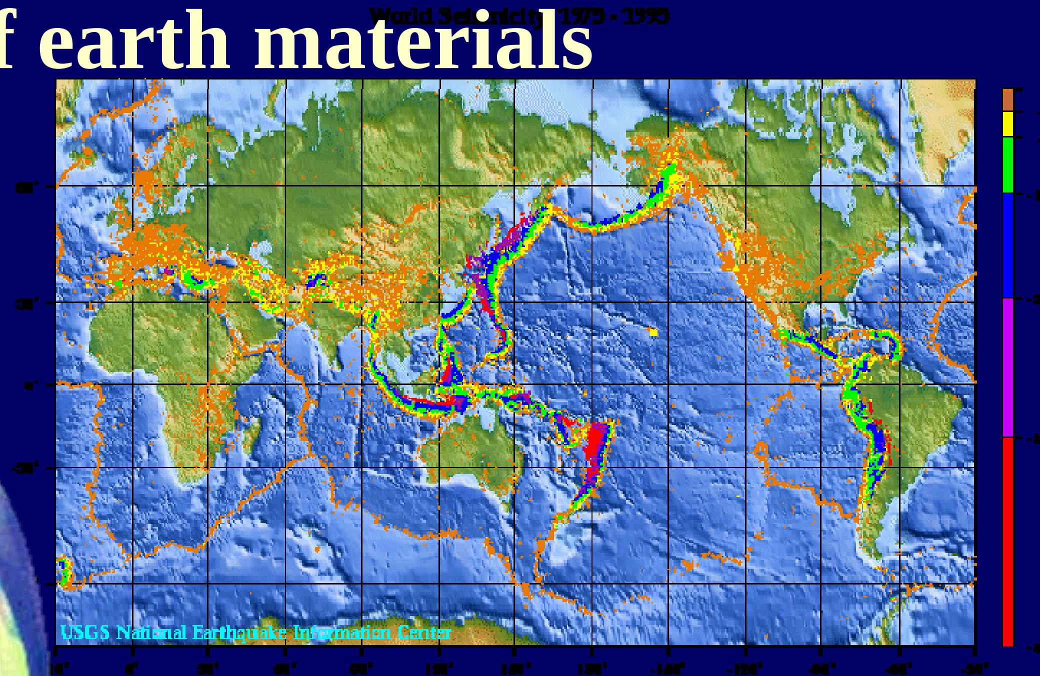

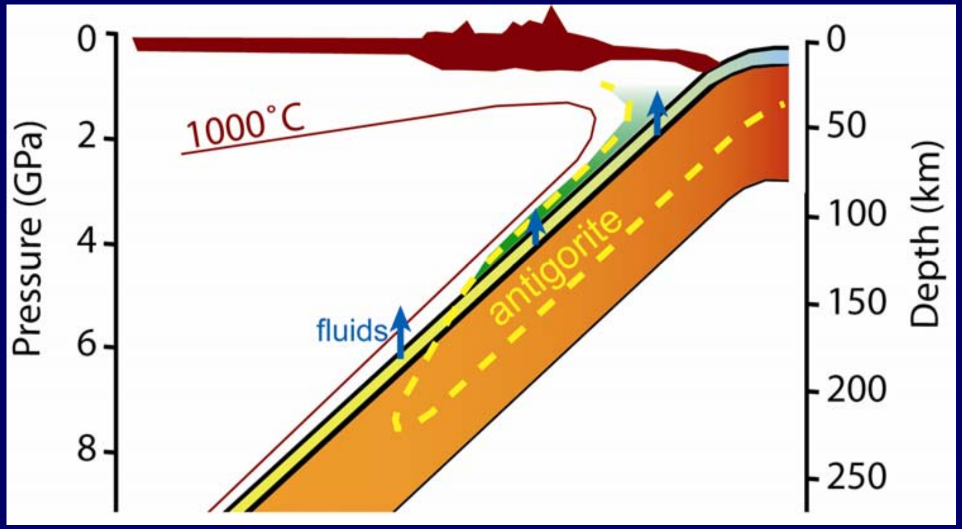

High P-T deformation on serpentinite

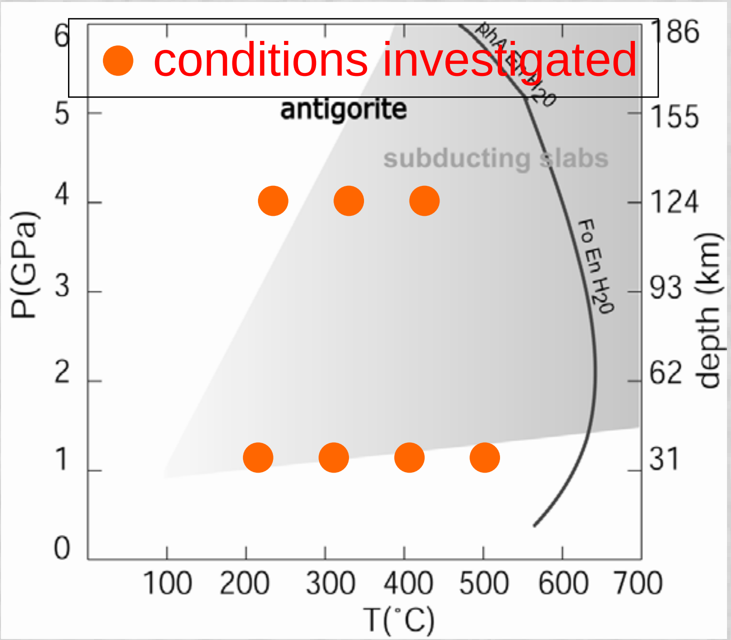

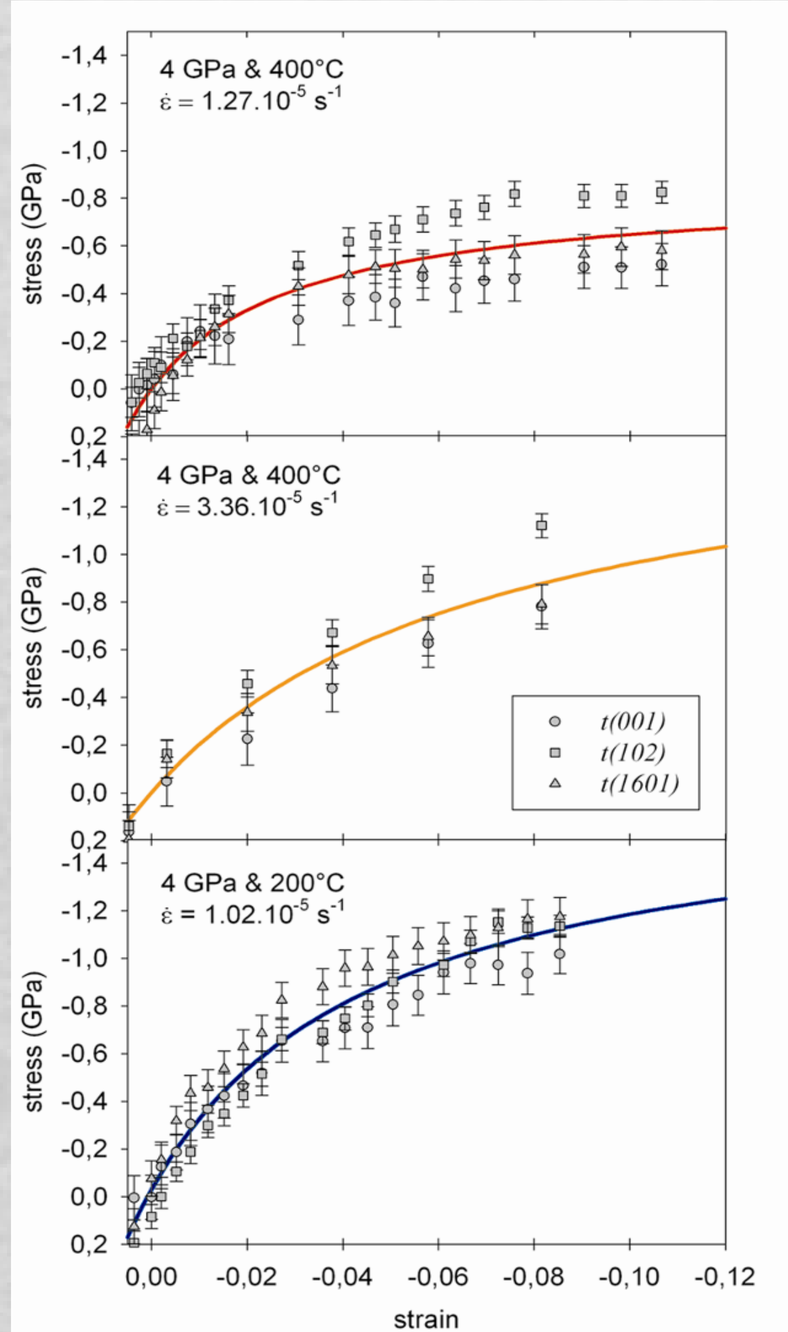

$d\varepsilon/dt$ fixed ~ 10^{-6} to 10^{-4} s^{-1}

14 deformation cycles

Hilairet et al, Science, in press.

Serpentine: weakest link at slab-mantle interface

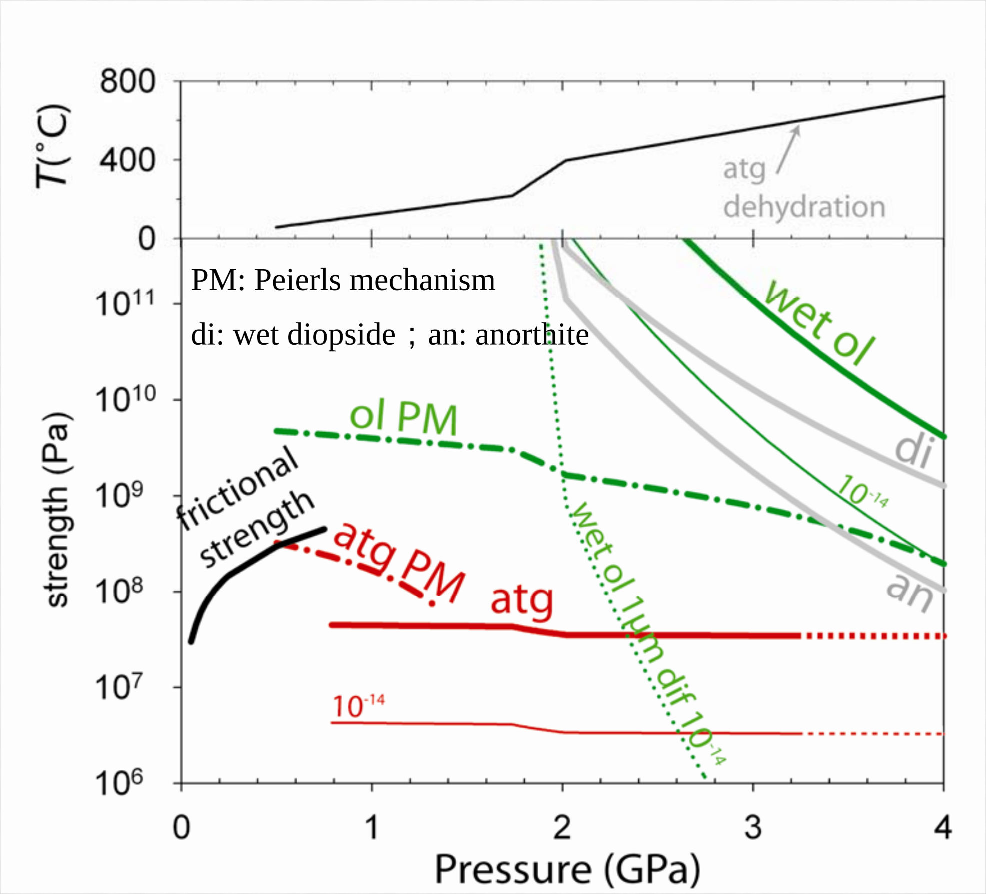

Hilairet et al, Science, in press.

$$\dot{\varepsilon} = A\sigma^{n}exp(-Q/RT)$$

$\dot{\varepsilon}$: strain rate
A: constant
σ: ultimate strength
n: stress exponent

- *Serpentine:*
  - *impedes stress build-up*
  - *limits downdip propagation of large earthquakes*

Comparison between mechanical data of hcp-Fe at ~18 GPa and deformation map of hcp-Zn

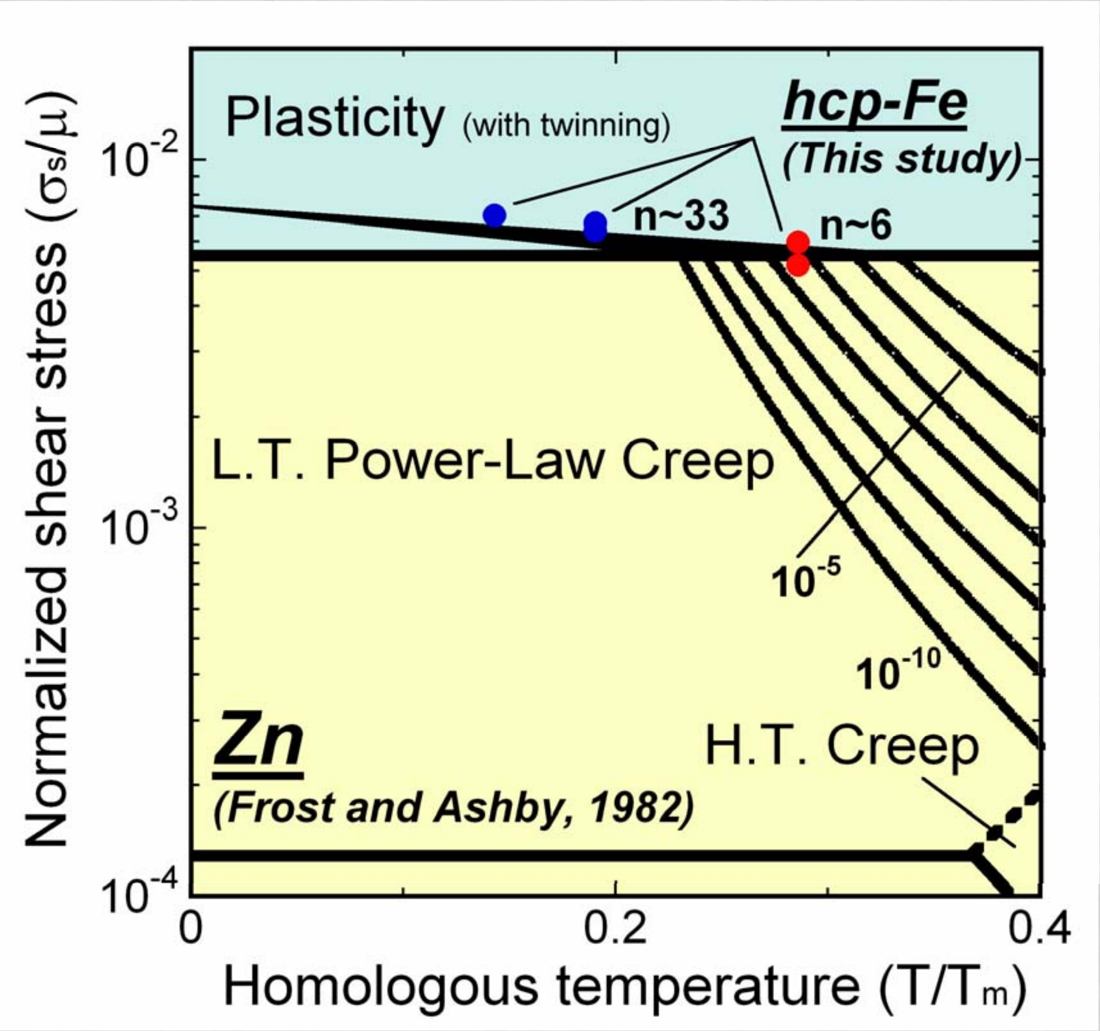

hcp-Fe

T_m at 18 GPa
= 2100 K
(Shen et al., 1998)

μ at 18 GPa
= 174 GPa
(Vocadlo et al., 2003)

Nishiyama et al., GRL, in press

Slip systems and lattice preferred orientation in deformed $CaIrO_3$ post-perovskite

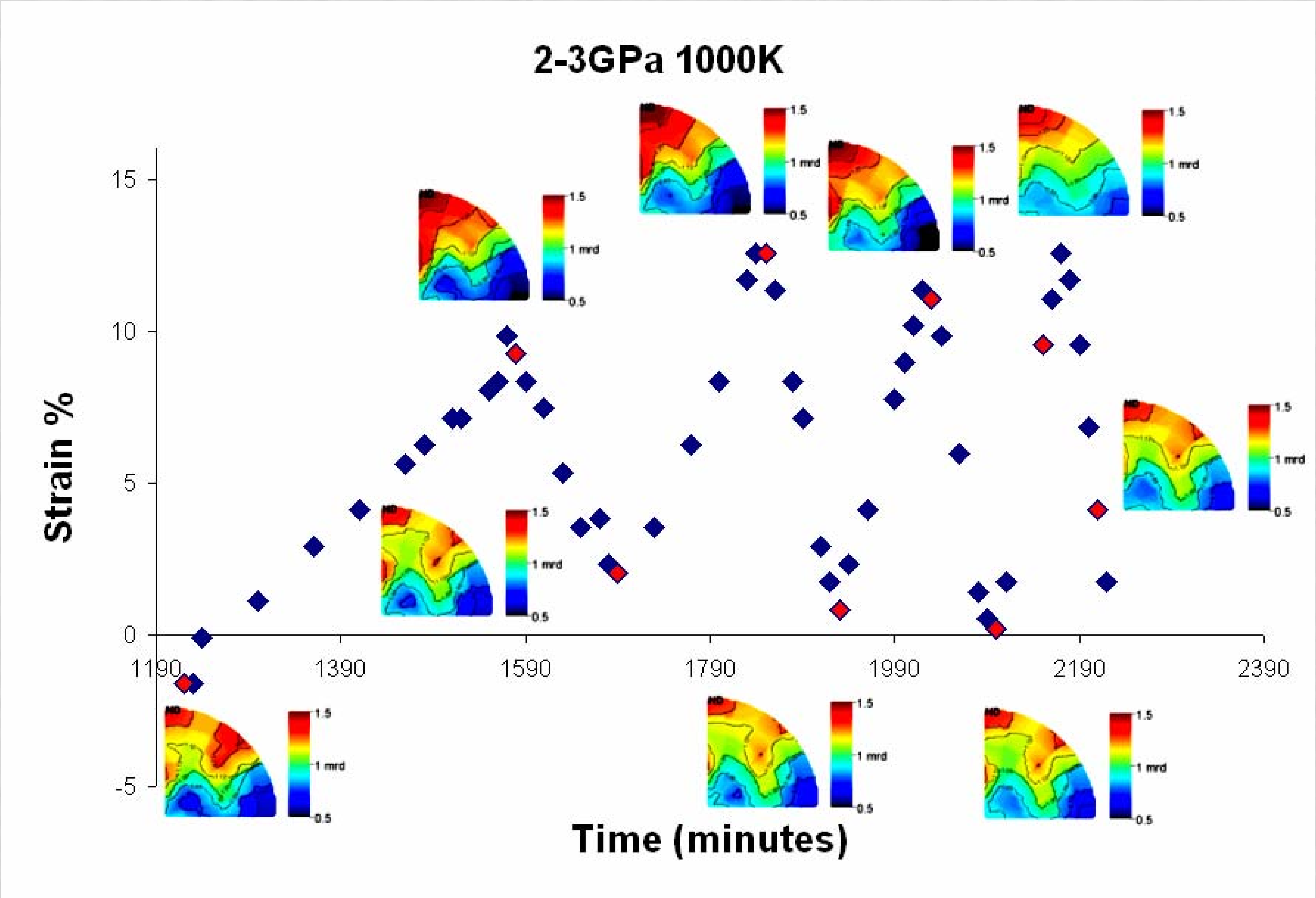

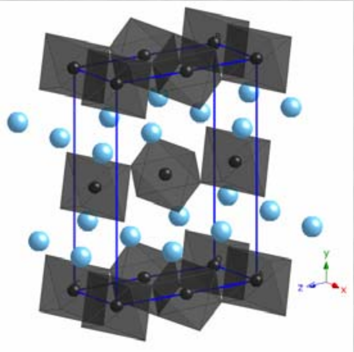

[100](010)

Not [001](110) as in $MgGeO_3$

Miyagi et al., EPSL,in press

The megabar LVP

- Megabar pressure generation with second-stage SD anvils (6/8) and 6/2 configuration on mm sized samples
- Load capacity: 1000 ton (10 MN)
- Operated with and without synchrotron radiation
- Structural studies under these conditions
- Deformation on large samples at transition zone P-T conditions
- Acoustic emission on large samples with controlled deformation

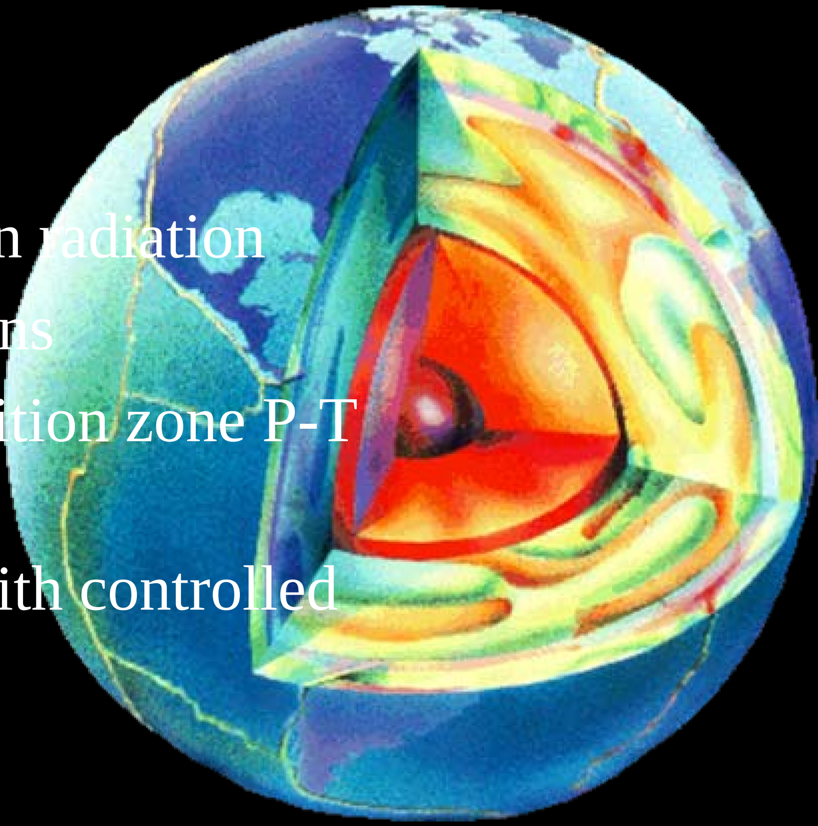

Modified Cubic-Anvil Apparatus

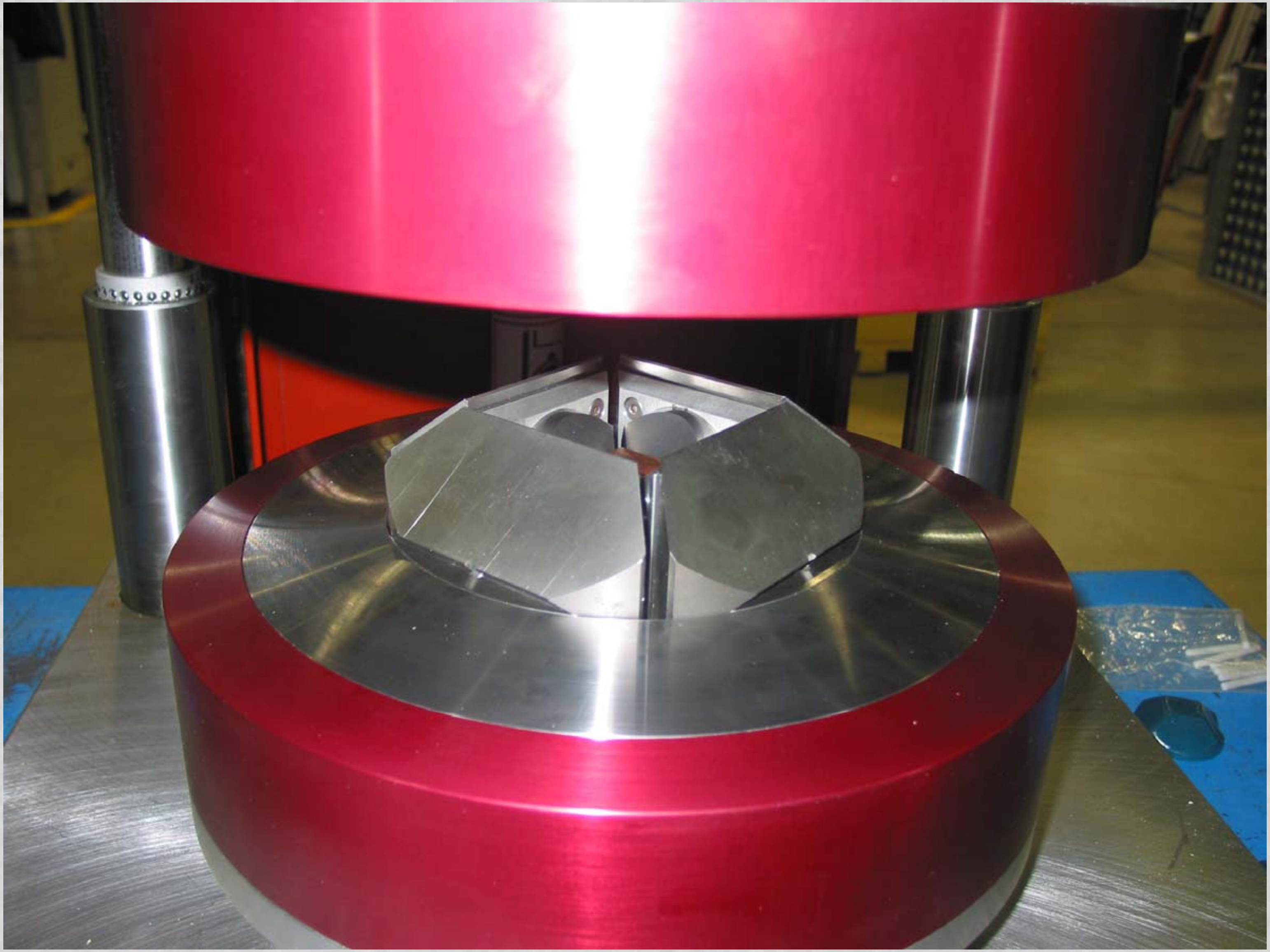

DDIA-30: a hybrid megabar module

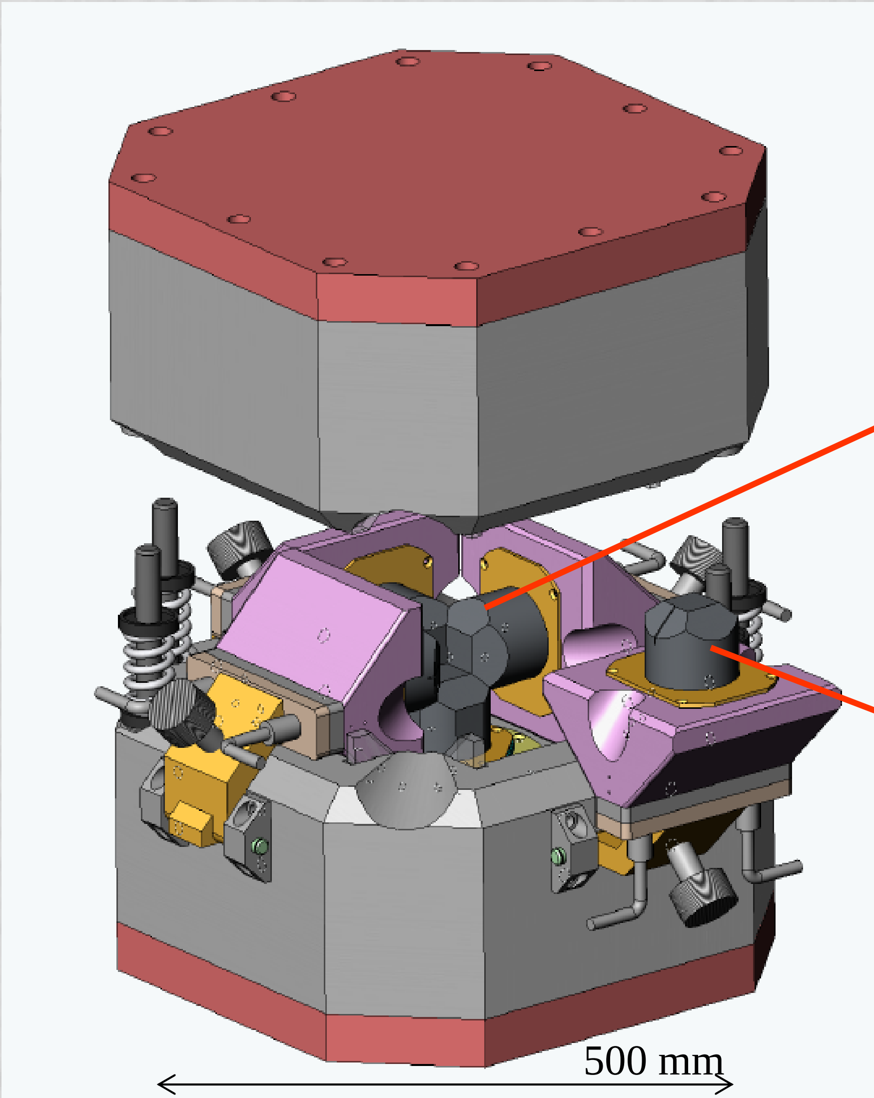

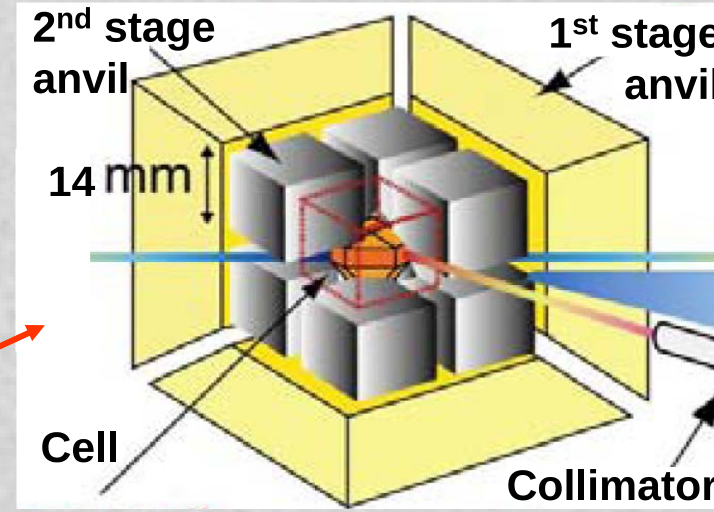

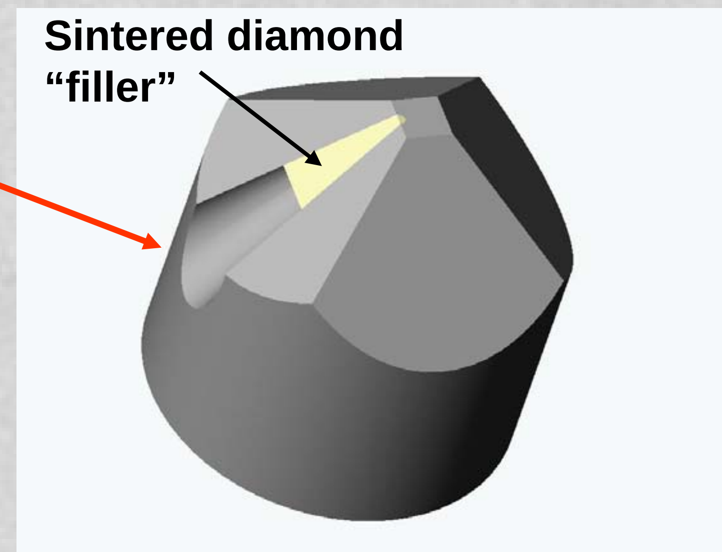

Conclusions

- Unique high pressure devices for wide range applications
  - T-25: 30 GPa, 2800 K
  - T-10: 23 GPa, 2000 K, SD anvils
  - DIA: 12 GPa, 2000 K,
  - D-DIA: 20 GPa, 1500 K, strain rates down to 10^{-7} s^{-1}
  - High-P topmography
- Continuing to develop new devices to take advantage of bright radiation sources
  - Modified cubic anvil apparatus for double-stage, ultrahigh pressure generation
  - D-DIA 30 for double-stage, ultrahigh pressure generation, deformation of large samples, acoustic emission
  - PE cell for structural studies of liquids
- Beamtime contact: wang@cars.uchicago.edu
- Post-doc opportunities